# SELF-ASSEMBLED PROTEIN BASED MATERIALS AND THEIR APPLICATIONS

Nistikakis Georgios

# Contributors – Acknowledgements

Firstly, I want to thank Professor Anna Mitraki for teaching me, guiding me, trusting me, and giving me the opportunity to work in her laboratory. For their contribution/advisory and participation in my evaluation, I want to thank Prof. Michael Kokkinidis and Dr. Kyriacos Petratos. I owe big gratitude and special thanks to Dr. Chrysoula Kokotidou for her endless help, teaching and advisory in the lab. I want to thank our lab members consisted by Dr. Graziano Deidda M.Sc. Chrysa Apostolidou, M.Sc. Petros Divanach, Ms. Marita Vasila, Ms. Konstantina Mitropoulou, Ms. Stella-Afroditi Mountaki, Mr. Giorgos Simatos, Ms. Marietta Alexaki, Ms. Rena Fanouraki for their collaboration, help and advisory during experiments. I also want to thank M.Sc. Georgianna Kontogianni for her contribution and support throughout this program. For their excellent technical support, I want to thank Prof. Giorgos Chalepakis, Ms. Aleka Manousaki, Mr. Stefanos Papadakis, and Ms. Eva Papadogiorgaki.

This thesis is dedicated to my family and especially my sister and mother and close friends for their endless and selfless support.

# Table of Contents



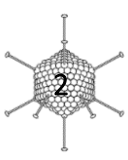

# Abstract

This work focuses on the design, production and structural characterization of the recombinant protein Bio-S and its amyloid fibrils for use in tissue engineering, as biomaterials. Briefly, in this work the design and the heterologous expression of the recombinant protein Bio-S is shown, through PCR cloning, utilizing an already studied construct as a base. Also, the production and purification of the protein by affinity chromatography, as well as, its "re-naturation" and self-assembly into amyloid fibrils. Subsequently, chemical and optical characterization of these fibrils was conducted in order to ascertain their conformation and properties. Finally, the functionalization of the amyloid fibrils with gold metallization was attempted as application proof-of-principle and was observed by electron microscopy.

More specifically,

In the beginning the basic characteristics and properties of amyloid fibrils and their applications as biomaterials are stated. Then, the fiber of adenovirus is presented as a self-assembly model and the production of the recombinant protein MetShaft61.Bio-S was designed in order to combine the self-assembly ability of MetShaft61 into amyloid fibrils, with the advantages of a histidine tail and a 16-peptide that can bind biotin. Demonstration of the aim of this work follows, explaining the design of Bio-S, based on MetShaft61, and the main followed strategy for its production. Lastly, the technique and reason of functionalizing the amyloid fibrils with gold nanoparticles is explained.

Materials and methods analysis follows, by mentioning every reagent, solution and mixture used and describing processes and protocols followed. Subsequently, the processes of amplification of the gene of interest by PCR, its excision and insertion into the proper plasmid and the transformation of E. coli cells with it via heat shock are described. The processes of overexpression of the Bio-S by IPTG, isolation after cell lysis and purification by affinity chromatography follow. Moreover, , the protocols for characterization techniques through electron microscopies and methods for validation of the products by immuno-recognition and agarose and polyacrylamide gel electrophoresis are showcased and analyzed.

Demonstration of the results follows, by evaluating cloned and cut products electrophoresed on agarose gels and expressed and purified products electrophoresed on polyacrylamide gels. Then, the results of immuno-staining Bio-S for biotin and histidine tag detection are presented, followed by amyloid fibril detection by Congo Red dying. Lastly, evaluation and commentary of the images taken with FESEM and TEM microscopy is done, and reaching and drawing the overall conclusions.

# Introduction

Biotechnology belongs to a broad area of biology, in which living organisms, cells and their components as well as biological systems and processes are researched for the development of technologies, tools and products, in fields like research, industry, environment, agriculture and medicine[1][2]. Tissue engineering is an interdisciplinary field that combines the principles of biology, engineering and material science in order to improve or replace the whole or parts of the tissue(i.e. skin, bone, etc.). The aim is to understand the basic functions of normal and pathogenic tissues and control cell and tissue responses to injuries and natural stimulators as well as the interactions with biomaterials, through chemical, pharmacological, mechanical and genetic modification handling[3].

As defined by the American National Institutes of Health, biomaterial is: "any substance or combination of substances, other than drugs (synthetic or natural in origin), which can be used for any period of time, and can augment or replace (partially or totally) any tissue, organ or function of the body, in order to maintain or improve the quality of life of the individual[4]". Therefore the extensive and continuous research on the development and use of biomaterials is considered of major importance for tissue engineering.

Mimicking natural and biological functions, materials and their properties has always been one of the best and most efficient approaches in developing biomaterials, techniques and systems for biotechnology. Studying and understanding of the mechanical and chemical properties and inherent abilities of biological materials is the key for such an approach. Thorough studying of organisms and cells derivatives and components, as well as their rational modifications have brought to light a vast amount of useful 'tools' for countless applications; from hyper-molecular biostructures, organelles, biofibers to oligo-peptides, proteins and nucleic acids and their vast range of properties, functions, structures, interactions, etc[5][6].

Recently, amyloid fibrils and their intrinsic properties have attracted the focus of interest for the development of biomaterials that can be applied in the tissue engineering area. Studies revealed the complexity, stability, unique inherent abilities of these supramolecular assemblies, thus giving them prospects for multi-functional applications[7].

# I. Theoretical background

## I. I. Amyloid fibrils

Proteins are essential building blocks of a cell's environment and take part in a variety of cell's chemical reactions. In order for a protein to assume its functional or structural role, it should acquire its specific conformation and proper folding. Under various circumstances, some proteins fail to assemble properly into their unique fold and they aggregate into highly ordered fibrillar assemblies, termed amyloid fibrils [8]. Amyloid fibril formation is associated with serious cellular malfunctions that lead to pathological disorders such as Alzheimer's disease [9], Parkinson's disease [10] and diabetes type II [11]. In some cases, such fibrils are produced and functionally used by organisms, such as the curli fibrils formed in E. coli, Salmonella and other bacteria[12], melanosomes (pmel) formed in mammalian melanophores[13] and many more[8][14].

Amyloid fibrils are structures, comprised by amino acid sequences that form distinctive beta sheet conformations (cross-β), that tend to self-assemble into long fibril like structures. Every mature fibril is a quaternary hyper-molecular structure, usually consisting from several protofilaments packed one next to the other, presenting high structural polymorphism, dependent mainly from the main-chain protein interactions (beta sheet hydrogen bonds) and secondarily from side-chain (hydrophobic interactions, hydrogen bonds, Van der Walls). Every protofilament's diameter is usually around 6-12Å wide, consists of thousands of proteins arranged in crystal like pattern, perpendicular to fibril axis and forming two parallel beta sheet conformations (characteristic intersheet distance approximately 10Å). Beta strands of each protein (characteristic interstrand distance approximately 4,7Å) are aligned perpendicular to the fibril axis and form a strong network of hydrogen bonds parallel to the fibril axis[8][15][16].

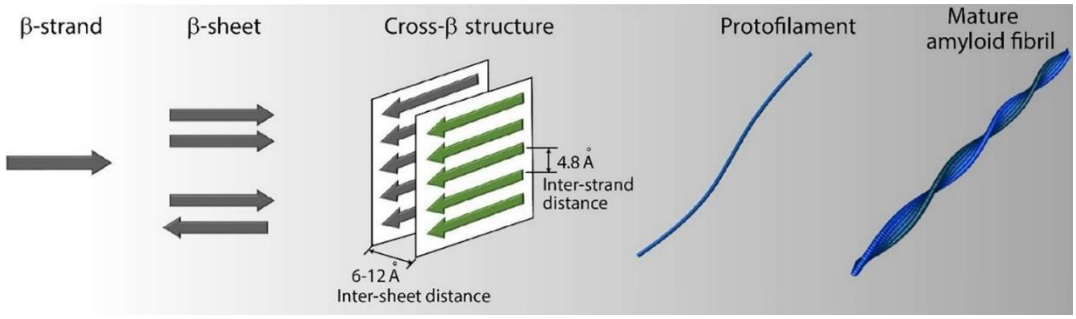


*Figure 1: Stages of amyloid fibril formation from secondary to quaternary level of structure. Beta strands take either parallel or antiparallel ß-sheet form, that spontaneously organize into cross-ß structures. Accumulation of these structures self-assemble into proto-filament, that over time tend to form mature amyloid fibrils[16].*

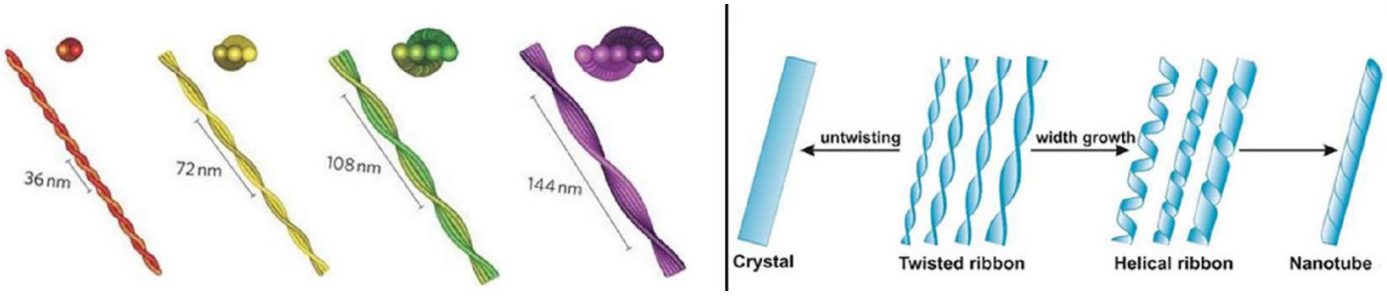


*Figure 2: Increase in the number of protofilaments per fibril can give increased width twisted-ribbon fibrils (left); Untwisting twisted-ribbon fibrils results to amyloid crystals, or grow of their width can result in helical ribbons and further evolve into nanotubes (right)[16].*

Their high organizational order and structure, as well as the plethora of hyper-molecular attractive interactions they consist of, makes amyloid fibrils i) extremely strong and resilient, having mechanical properties comparable to steel, ii) thermodynamically stable, and iii) resistant to chemical and biological degradation[8][15][16].

Optical observation of amyloid fibrils by microscopy is a typical method for their characterization. Electron microscopy, like Field Emission Scanning Electron Microscopy (FESEM) and Transmission Electron Microscopy (TEM), as well as Atomic Force Microscopy (AFM), can provide high resolution, nano-scale images and have proved to be important techniques to measure and observe the conformation, architecture and magnitude of the amyloid fibrils[8][15].

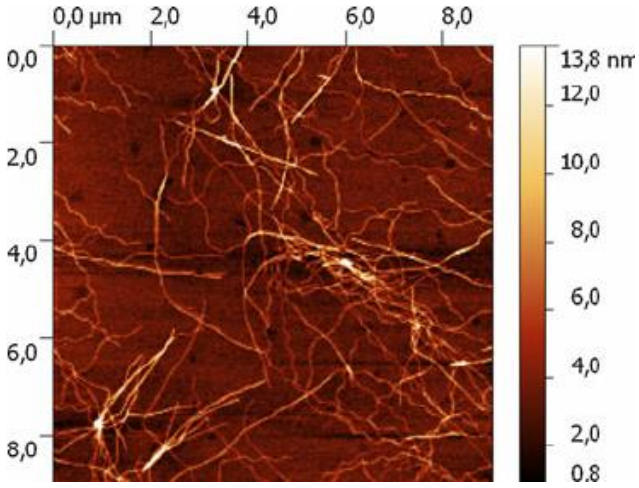


*Figure 3: Atomic force microscopy topography of insulin amyloid fibrils[17].*

X-ray fiber diffraction of aligned fibrils can provide structural information and precise distance measurements among lateral levels. X-ray diffraction on amyloid fibrils is considered a typical method to detect the characteristic cross-β conformation, where a distinct cross beta diffraction signal appears in the equator (corresponding to fibril's intersheet (around 10Å) spacing) and in the meridian (corresponding to fibril's interstrand (around 4,7Å) spacing)[8][15].

Moreover, amyloid fibrils can be easily detected by amyloid binding dyes such as the sodium salt Congo Red and benzothiozole salt Thioflavin T. When excited at 450nm, unbound Thioflavin T emits around 527nm, but once bound to amyloid fibrils, a strong fluorescence signal is produced at 482nm. Basic Congo Red aqueous solution (pH ≥ 5.2) has a deep blood red hue, that once is bound to amyloid fibrils, its absorbance peak shifts from 490nm to 512nm, while producing a relative maximum emission at 540nm. When placed under polarized light, Congo Red stained amyloid fibrils exhibit a characteristic birefringence, that shifts its red colour to apple green-yellow[18].

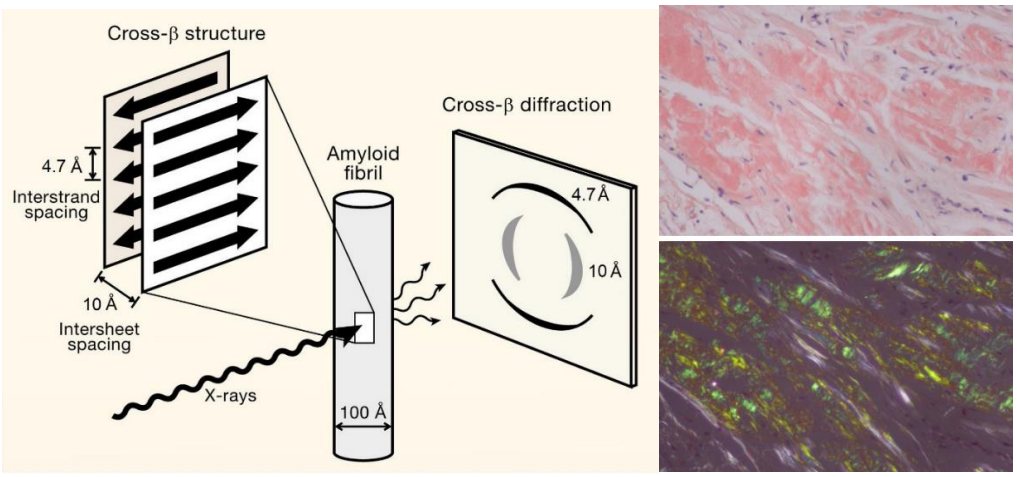


*Figure 4: Fiber x-ray diffraction to amyloid fibrils gives the corresponding distinctive cross beta diffraction pattern (left figure)[19]. Right: Congo red stained amyloid fibrils (red colour) of cardiac tissue with systemic amyloidosis (top) and the characteristic apple green-yellow birefringence it exhibits under polarized light (x400 original images)[20].*

## I. II. Amyloid fibrils as biomaterials

A wide range of synthetic and natural materials can be used as biomaterials, scaffolds and surfaces for tissue engineering. Generally, in order to be used as biomaterials and be able to safely interact with cells, biomolecules and tissues, materials need to fulfil some requirements, such as:

i) high biocompatibility and non-toxicity,
ii) chemical stability (e.g. Sterilizable without changes in form and composition) and/or biodegradability in non-toxic products,
iii) mechanical properties suitable to the tissue it simulates or supports,
iv) sufficiently long shelf-life[21].

As previously mentioned, due to their highly organized architecture and strong hyper-molecular stability, amyloid fibrils exhibit suitable biomaterial properties, such as mechanical strength, chemical and biological stability. Their self-assembly ability and natural origin gives them advantage against other materials and assures their high biocompatibility. The

polymorphism of amyloid fibrils derives from their amino acid sequence, meaning that by specific changes in their sequence one is able to tune their conformation, architecture and mechanical properties for wide range of application. Furthermore, by introducing proper sequence mutations to certain positions, additional abilities and properties can be given to amyloid fibrils (e.g. metal binding). Therefore, a vast amount of amyloid fibrils applications has emerged in tissue engineering, including:

- Scaffolds for cell support, growth and direction[22]-[24]
- Targeted drug and gene transfer carriers[25]-[27]
- Nanocircuits and electronics as metal nanoparticle templates[28][29]
- Inorganic bio-mineralization ($Ca^{2+}$)[30]
- Environmental applications (capturing Cs and $CO_2$)[31][32]
- Platforms for biosensors and minimal versions of enzyme catalysts and more[33].

## I. III. Fiber of adenovirus type 2 as self-assembly model

Fibrous proteins are a significant part of structural biology, found in a huge number of biological materials and tissues. Many viruses and phages are using fibrous structures as anchors and bridges to attach and infect their host cells. Adenovirus type 2 is medium size (90-100 nm) non-enveloped virus with unique fiber proteins projected out of its capsid. Its icosahedral nucleocapsid contains its double stranded DNA genome. One fiber protein protrudes from each of the 12 vertices[34][35].

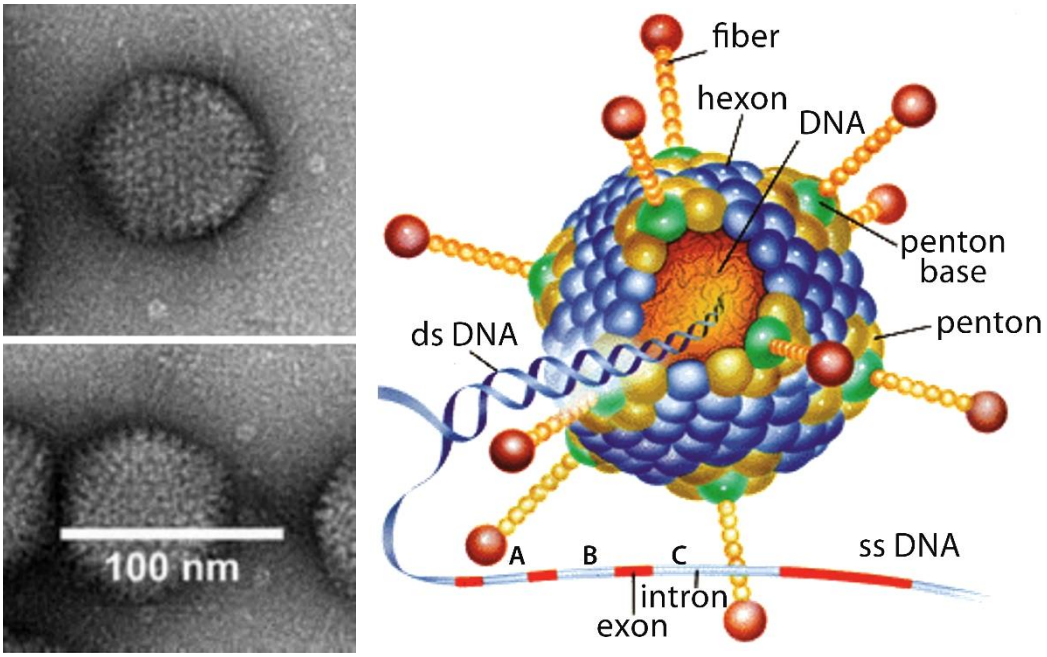


*Figure 5: Transmission electron microscopy images showing adenovirus virions' size, capsid structure and fibers (left) [36], Illustration of adenovirus virion (right)[37].*

Its 20 faced capsid consists of two main proteins called hexons and pentons respectively. Hexons are placed in the center of every triangle shaped face. The icosahedral virions have 12 vertices, containing a penton base and the fiber attached to it. [34][35].

The adenovirus fiber protein is composed of the shaft (main fiber body) anchored on a penton base of virion capsid, projecting outwards and a distinct globular head, at the tip of the shaft, that interacts with the host cells' Coxsackie and Adenovirus Receptors (CARs)[36]. Every fiber is a homo-trimeric protein, where each monomer spirals with the other two forming a tightly packed fiber. Each homo-trimer comprises a globular head, a long fibrous shaft body, and a tail anchored to the penton base of the capsid. The homo-trimer globular head is responsible for the docking and activation of CAR cell receptors, that triggers the virion endocytosis[38]. Studies have shown that elimination of capsid as well as the penton, allows transfer by attachment to CAR receptor, but internalization through an unknown mechanism[39].

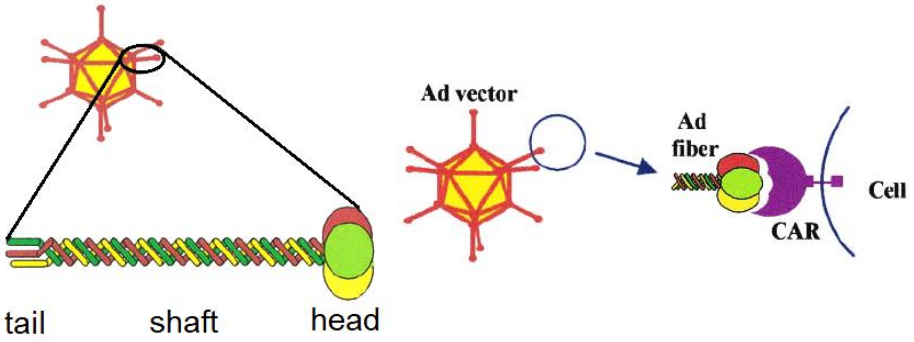


*Figure 6: Adenovirus fiber homo-trimer illustration (every colour represents a different monomer) (left) and binding to the CAR receptor (right) [40].*

Adenovirus fiber is an approximately 35nm hyper-molecular structure and as mentioned before is a homo-trimeric structure, where every monomer contains 582 amino acids and is composed of three distinctive areas, the C-terminal knob, the fibrous spiral shaft and the N-terminal tail. The globular head is not only responsible for CAR receptor binding, but also for the self-assembly of the fiber in its trimeric state. The shaft, the main body of the fiber, is about 30nm long and consists of 22 pseudo-sequence repeats made out of hydrophilic and hydrophobic amino acid sections, with an exposed loop connecting them. Two beta strands with a beta turn in the middle are formed, where one is parallel and the other one is $45^{o}$ angle to fiber's axis, followed by a loop. A dense network of hydrogen bonds, as well as ionic bridges, reinforce the conformation of this structure conveying high chemical and mechanical stability[41].

There have been many studies, where adenoviruses are used as vectors for cell targeting and development of gene therapy techniques and drug delivery systems. These include modifications of the homo-trimeric globular head (increased probability of attachment),

replacement or addition of other virus fibers (different receptor targeting) to penton bases, as well as molecule/complex addition (specific cell/receptor targeting) on the fiber head or around the virion capsid[42]-[44].

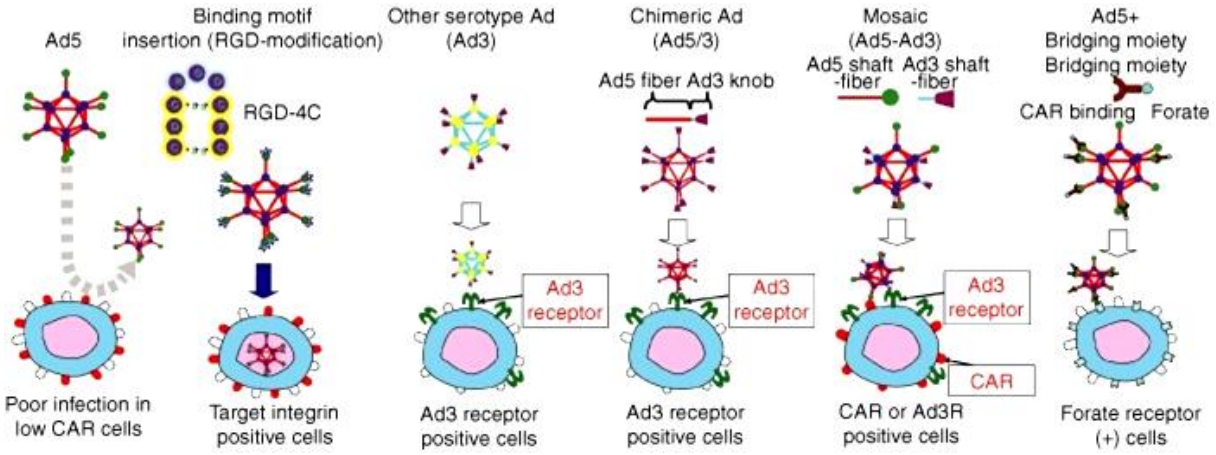


*Figure 7: Modification of adenovirus for CAR- independent transduction. Such modifications include fiber modification, switching between serotypes, chimeric or mosaic fiber placement, and molecule-based targeting[44].*

Other studies have aimed to utilize isolated aden ovirus fibers and recombinants variants of them, as drug/nucleic acid delivery carriers. Replacement of fiber's globular head with other trimerization motifs, like the C-terminal of the fibritin's phage T4, can produce a recombinant, hybrid homo-trimeric conformation of the fiber, with enhanced chemical stability as well as higher expression yield[45]-[48].

Absence of the globular head or any other trimerization motif results to amyloid fibril formation resulting to a completely different self-assembling conformation and architecture[41]. Previous studies have shown that the GAITIG peptide is the shortest sequence responsible for amyloid aggregation of the adenovirus fiber sequences[48]. The pentapeptide GAIIG has also been shown to be a small self-assembling block, found in amyloid fibrils of Alzheimer's disease and HIV-1 V3 loop of gp120 protein[49]. Based on these minimal self-assembling building blocks many oligo- and polypeptides can be designed and synthesized, forming amyloid fibrils with a vast range of structural conformations, chemical properties and abilities targeted for a plethora of tissue engineering applications[22][25][29][30].

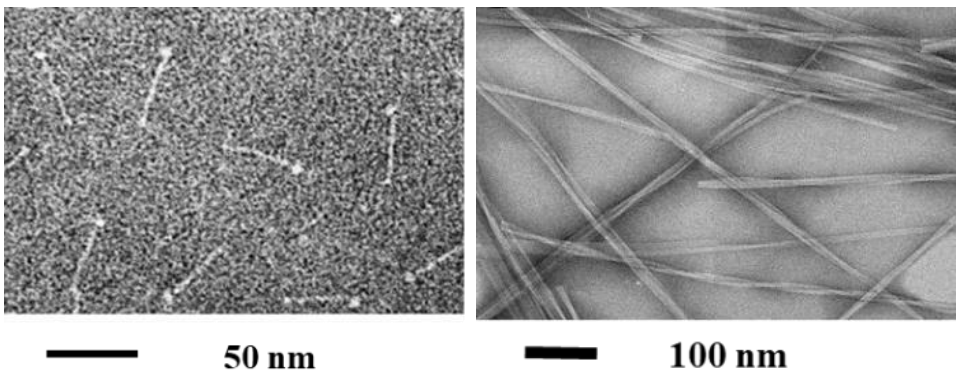


*Figure 8: Transmission electron microscopy images of adenovirus fibers (left) and amyloid fibrils (right)[41][50]*

## I. IV. Protein inspired from the adenovirus fiber - MetShaft61

A recombinant protein has been previously designed, produced and studied in our lab. MetShaft61 is composed of a 332 aa, starting from Methionine 61 (61-392 aa) of the natural shaft, with molecular weight Mw:34,38295 kDa and isoelectric point pI:7,77. The globular head was removed[51].

```
     61          71          81          91          101         111
     |           |           |           |           |           |
  61 MLALKMGSGL TLDKAGNLTS QNVTTVTQPL KKTKSNISLD TSAPLTITSG ALTVATTAPL 120
 121 IVTSGALSVQ SQAPLTVQDS KLSIATKGPI TVSDGKLALQ TSAPLSGSDS DTLTVTASPP 180
 181 LTTATGSLGI NMEDPIYVNN GKIGIKISGP LQVAQNSDTL TVVTGPGVTV EQNSLRTKVA 240
 241 GAIGYDSSNN MEIKTGGGMR INNNLLILDV DYPFDAQTKL RLKLGQGPLY INASHNLDIN 300
 301 YNRGLYLFNA SNNTKKLEVS IKKSSGLNFD NTAIAINAGK GLEFDTNTSE SPDINPIKTK 360
 361 IGSGIDYNEN GAMITKLGAG LSFDNSGAIT IG                             392
                           First amino acid  Last amino acid
```

MetShaft61 has been successfully expressed *in E.coli* and proved to be able to self-assemble into amyloid fibrils. The abundant production of this protein resulted in the formation of a dense network of amyloid fibrils with fibrous architecture, that can be used as a scaffold for cell attachment and proliferation towards tissue engineering purposes[51].

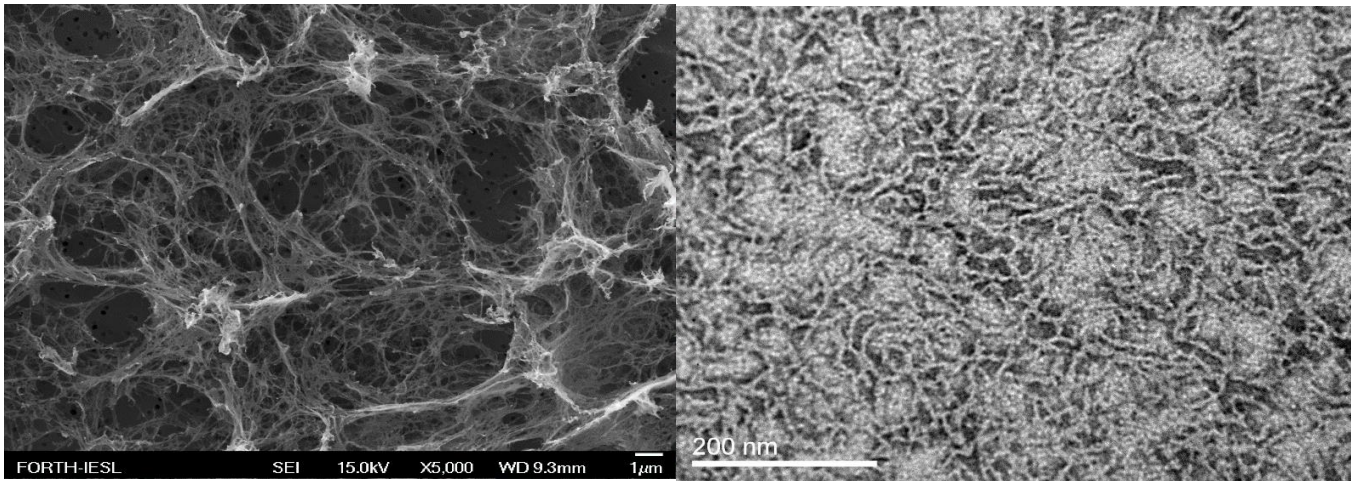


*Figure 9: Scanning electron microscopy images (left) and Transmission electron microscopy images (right) of MetShaft61 amyloid fibrils ( 0,5mg/ml Metshaft61 in 20mM ethanolamine)[51]*

## I. V. Aim of the present work

The present thesis focuses on the development of a protein that can produce amyloid fibrils in a conformation and architecture that can be potentially used as scaffold in tissue engineering, support of cell growth and/or serve as an implant or platform for detection (e.g. biosensor). Such scaffolds are essential to possess a plethora of properties and be multifunctional. For instance, they should not just support cell growth but also be able to induce certain cell responses (e.g. differentiation). This can be achieved by designing recombinant proteins with sites that can be "decorated" with molecules (e.g. cytokines) or atoms/ nanoparticles (e.g. metals) serving in a wide range of applications.

The aim of this work was the design and production of a new recombinant protein based in the MetShafts61 sequence, thereafter named Bio-S. Bio-S was designed in order to combine the self-assembly ability of MetShaft61 into amyloid fibrils, with the advantages of a histidine tail and a 16-peptide that can bind biotin. Moreover, the protein's potential applications are being explored through the functionality conveyed by its modifications.

Specifically, the addition of a histidine hexa-peptide and a biotin binding 16-peptide at the N-terminus of the MetShaft61 sequence was achieved with the use of the appropriate plasmid. Poly-histidine tail has a high affinity to metals like copper, nickel, and zinc, so it can be used as a metal binding site. His-tag addition to a recombinant protein usually serves as an easy affinity purification method, when it bounds to Nitrilotriacetic acid (NTA) seeded beads through $Ni^{2+}$ coordination. By the same principle, any desirable NTA seeded molecule can be attached by the His-tag of the recombinant protein. His – tagged proteins are also resistant to degradation, making them ideal parts of drug/gene delivery proteins [52].

Biotin and biotinylated molecules have an extremely high affinity to avidin and streptavidin and the bond they form occurs rapidly and is the strongest noncovalent bond known in nature. Thus, formation of biotin – streptavidin – biotinylated-molecule complexes is a common strategy for attachment of any desirable molecule on a protein. A site on the protein that can bind biotin, can convey to amyloid fibrils advantageous properties and prospects for a wide range of biotechnological applications (e.g. binding of cytokines or drugs)[53][54].

The S-G-L-N-D-I-F-E-A-Q-K-I-E-W-H-E sequence is a 16-peptide that can be recognized by a birA enzyme and allow biotin attachment through its lysine. BirA is a trigger enzyme that functions as a ligase to biotin-lysine conjugation, as well as a regulator of biotin gene expression. This biotinylation process has already been shown to work successfully in the cytoplasm of a bacterial cell, while the protein is produced[54][55]. The advantages of this *in vivo* biotinylation are i) comprehensive and uniform biotinylation of the proteins, ii) avoidance of subsequent separation and purification of the modified ones, iii) removal of birA enzyme. This process requires the simultaneous production of birA enzyme in the bacterial cells, thus, the insertion of a birA plasmid, the simultaneous production of the ligase with the expressed protein and the presence of the biotin in the cells[53][54].

## I. V. a. Studied protein: Bio-S

Successful design and production of the proper plasmid vector can heterologously over-express Bio-S in *Escherichia Coli.* Bio-S is expected to have a sequence of 371 amino acids, with Molecular Weight Mw:38,85k Da and theoretical isoelectric point pI:6,5.

```
    1          11          21          31          41          51
    |          |           |           |           |           |
  1 MGSSHHHHHH SSGLVPRGSH MSGLNDIFEA QKIEWHEEFM LALKMGSGLT LDKAGNLTSQ   60
 61 NVTTVTQPLK KTKSNISLDT SAPLTITSGA LTVATTAPLI VTSGALSVQS QAPLTVQDSK  120
121 LSIATKGPIT VSDGKLALQT SAPLSGSDSD TLTVTASPPL TTATGSLGIN MEDPIYVNNG  180
181 KIGIKISGPL QVAQNSDTLT VVTGPGVTVE QNSLRTKVAG AIGYDSSNNM EIKTGGGMRI  240
241 NNNLLILDVD YPFDAQTKLR LKLGQGPLYI NASHNLDINY NRGLYLFNAS NNTKKLEVSI  300
301 KKSSGLNFDN TAIAINAGKG LEFDTNTSES PDINPIKTKI GSGIDYNENG AMITKLGAGL  360
361 SFDNSGAITI G                                                      371
```

First amino acid | Histidine tag sequence | 16peptide sequence | MetShaft61 sequence | Last amino acid

## I. V. b. pET-28a-bio

Plasmid pET-28a-bio is a modified version of pET-28a-c(+) vector, where a 16-peptide biotin binding nucleotide sequence has been inserted between NdeI and EcoRI restriction endonuclease sites.

### pET-28a-bio sequence

AGAAGGAGATATACCATGGGCAGCAGCCATCATCATCATCATCACAGCAGCGGCCTGGTGCCGCGCGG
CAGCCATATGTCCGGCCTGAACGACATCTTCGAGGCTCAGAAAATCGAATGGCACGAAGAATTCGAGC
TCCGTCGACAAGCTTGCGGCCGCACTCGAGCACCACCACCACCACCACTGAGATCCGGCTGCTAACAA

NdeI site | EcoRI site | XhoI site | His tag | 16peptide of biotin | Start codon

The insertion of the MetShaft61 nucleotide sequence was designed to be placed between the restriction enzyme sites of EcoRI and XhoI. To do that both the plasmid and MetShaft61 DNAs should be cut at the restriction enzyme sites, with the corresponding enzyme and ligated through T4 DNA ligase. To increase the chances of successful ligation, plasmid vectors should also go through a de-phosphorylation process.

## I. VI. Functionalization of the amyloid fibrils by metallization with Gold nanoparticles

Gold nanoparticles are considered to be efficient delivery systems for nucleases and bioactive molecules for therapeutic purposes[56]. Their ability to scatter light intensely and absorb near infrared and X-ray radiation makes them ideal for diagnostic imaging. Thus, attachment of Au nanoparticles on the surface of amyloid fibrils can functionalize them towards a plethora of biological applications[57].

Taking advantage of this affinity of poly-histidine sequence to cations of nickel ($Ni^{2+}$), it is relatively easy to trap NTA conjugates on ahis-tagged protein. The 5 nm Ni-NTA Au nanoparticles (Nanogold) are designed for the detection or localization of Histidine (His)-tagged recombinant proteins in protein complexes, tissue or cell samples using transmission electron microscopy (TEM).

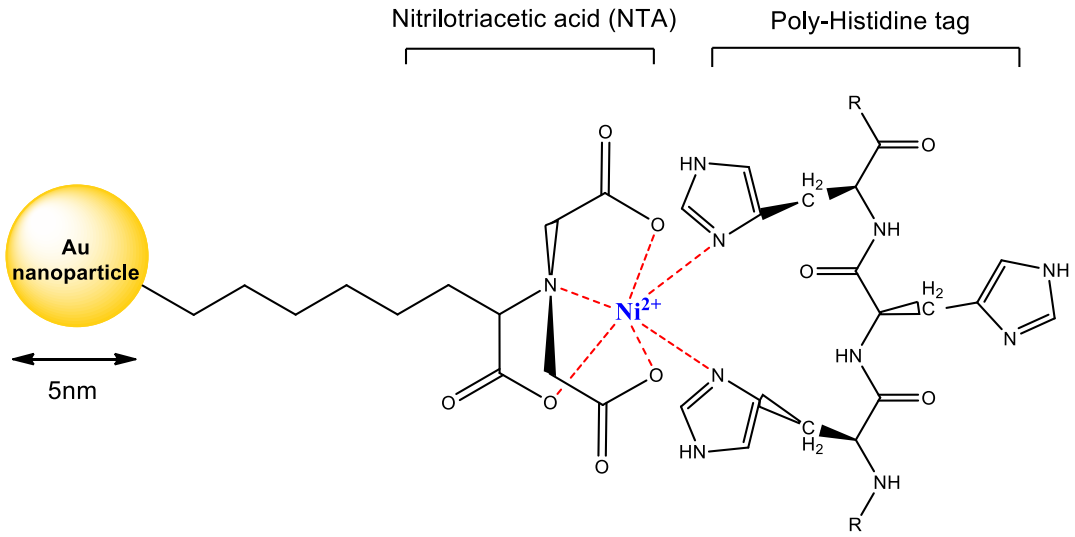


*Figure 10: Poly-histidine – $Ni^{2+}$ – NTA complex attached to 5nm Au nanoparticles*

# II. Materials and methods

## II. I. Materials

All materials and reagents were purchased from Sigma-Aldrich, unless otherwise stated

## II. II. Methods

### II. II. a. Design of the plasmid vector for Bio-S production

❖ Polymerase Chain Reaction (PCR)

Production of the recombinant protein Bio-S requires its DNA construction, specifically the incorporation of MetShaft61 gene in the proper vector.

A process like this requires the isolation of the gene of interest (MetShaft61 gene) from the vector of origin and its subsequent insertion to the vector of interest. Therefore, the amplification of the gene can be easily achieved by the method of polymerase chain reaction (PCR). PCR is a method of amplification of nucleic acid sequences, that uses the ability of DNA polymerase to synthesize new DNA strands complementary to the offered template strand. In order to do so, DNA polymerase needs primers, small nucleic acid sequences designed to be complementary to the beginning of the template strand, for polymerase to start adding nucleotides. This process provides exponential gene amplification through sequential cycles of three heating stages (n cycles of one double-stranded DNA molecule gives 2n dsDNA)[58].

i. Denaturation, where the double stranded DNA of interest separates (app. 94-96$^{o}$C)

ii. Annealing, where forward and reverse primers attach to separated DNA strands (60-70$^{o}$C) (depends from the melting point (Tm) of the primer, which depends from the length and percentage of CG/AT nucleotides)

iii. Elongation, where heat resistant DNA polymerase synthesizes the new DNA strand (about 70-74$^{o}$C)

❖ Primers

The forward primer was designed to have 22 nucleotides, 55% GC/AT ratio and melting temperature (Tm): 63°C, where the reverse one has 29 nucleotides, 52% GC/AT ratio and Tm: 63°C. The annealing was calculated to happen at 61°C with the use of Deep Vent DNA polymerase.

Forward primer (EcoRI): 5'-GGCCGAATTCATGCTTGCGCTT-3'

Reverse primer (XhoI): 5'-GCCCCTCGAGTCTATCCTATTGTAATGGC-3'

EcoRI site XhoI site

❖ Reaction

To ensure that the amplification happens to MetShafts61 gene and only and not non-specifically, two samples were prepared as well as one control without the addition of this gene.

| Control | Sample 1 | Sample 2 |
|---|---|---|
|  |  |  |
| +DNA polymerase<br>-MetShaft61 DNA | +DNA polymerase<br>+MetShaft61 DNA | +DNA polymerase<br>+MetShaft61 DNA |

For this reaction, reagents were added in the following order (reaction volume: 50 µl)

| Reagents | Volume |
|---|---|
| 10x Polymerase buffer | 5 µl |
| Sterile-distilled $H_2O$ | 40 µl (40,5 µl for control) |
| 10 mM dNTP mix | 1 µl |
| 100 mM MgSO4 | 1 µl |
| 20 µM Forward primer | 1 µl |
| 20 µM Reverse primer | 1 µl |
| DNA (MetShaft61) | 0,5 µl (except control) |
| Deep Vent polymerase | 0,5 µl |

PCR reaction was set for 30 cycles in the following sequence.

| PCR reaction | | | |
|---|---|---|---|
| PCR stages | | Temperature (°C) | Time |
| Initial denaturation | | 95 | 5 min |
| DNA denature | 30 Cycles | 95 | 30 sec |
| Annealing | | 61 | 30 sec |
| Elongation | | 72 | 90 sec |
| Final elongation | | 72 | 5 min |

Evaluation of the PCR product is important for the continuation of the experiments.

## II. II. b. Agarose gel electrophoresis

Agarose gel electrophoresis is a method that separates a mixed population of macromolecules. It is usually used for the separation of DNA or RNA fragments according to their length. Moreover, it is commonly used in order to evaluate and/or isolate the desired products from PCR and cut reactions.

A 1% w/v agarose in Tris-Acetate-EDTA (TAE) buffer (pH:8) mixture was prepared. The mixture was heated in a microwave until agarose was dissolved. Gel red stain (GelRed™ Nucleic Acid Gel Stain– BIOTIUM) was also diluted 10000-fold. The agarose gel was deposited in a horizontal electrophoresis apparatus, while the apparatus was filled with 1x TAE buffer.

For the evaluation of the PCR product, a DNA portion of each sample was mixed with Gel Loading Dye (New England Biolabs) and then loaded into the wells of the gel. A 2-log DNA ladder (New England Biolabs) was also mixed with the loading dye and loaded in the gel. An electric field of 80 V was applied until the samples entered the gel and then the voltage was increased to 100 V. Agarose gels were viewed using a UV-lamp, where UV light excites the gel red stain, which is bound to DNA, rendering the samples visible.

Samples that correspond to the DNA's molecular length, were isolated from the agarose gel and purified with a PCR clean up kit (Macherey Nagel).

## II. II. c. Double digest (cut) and de-phosphorylation reactions

After the successful PCR reaction, DNA product and plasmid vectors have to be cut with the same restriction endonucleases XhoI and EcoRI (High Fidelity).

PCR product (MetShaft61 DNA)

Plasmid Vector (pET-28a-bio)

For this reaction, reagents were added in the following order (reaction volume: 50 µl)

| Double digest reaction | | |
|---|---|---|
| **Reagents** | **PCR product** | **Plasmid vector** |
| DNA | 10 µl | 15 µl |
| Sterile-distilled $H_2O$* | 33 µl | 28 µl |
| 10x CutSmart buffer | 5 µl | 5 µl |
| XhoI | 1 µl | 1 µl |
| EcoRI – HF | 1 µl | 1 µl |

(XhoI, EcoRI – HF, CutSmart® buffer were purchased from New England Biolabs)

*After the $H_2O$ addition to DNA, the mixture was heated at 70°C for 10 min, then cooled down for 1 min on ice and spun down, before the addition of the remaining reagents.

When both restriction enzymes were added, the samples were incubated at 37°C for 30 mins to react. After 30 min, the samples were loaded to 1% agarose gel in the same process mentioned before and 80V of electric field was applied to achieve proper band separation. This process allows the isolation and extraction of clean DNA products from the agarose gel. Bands with the DNA of the corresponding MW are cut with scalpel from the rest of the gel, gel is melted and DNA is extracted from a series of processes described in plasmid extraction kit(Macherey Nagel).

Next, de-phosphorylation reaction of the plasmid vector pET-28a-bio follows, where reagents were added in the following order (reaction volume: approx. 20 µl)

| De-phosphorylation reaction | |
|---|---|
| **Reagents** | **Volumes** |
| DNA of pET-28a-bio | 19 µl |
| 10x Antarctic buffer | 2,2 µl |
| Antarctic phosphatase | 1 µl |

(Antarctic phosphatase and Antarctic buffer were purchased from New England Biolabs)

The reaction was conducted at 37°C for 15 min and then placed at 70°C for 5 minutes for heat-deactivation of the phosphatase enzyme. Then, the sample was cooled for 1 min on ice and spun down.

## II. II. d. Ligation reaction of MetShaft61 DNA and pET-28a-bio plasmid with T4 ligase

After measuring the concentrations of both DNA samples, with the Nanodrop instrument, the volumes of the proper ratio of plasmid to inserted gene was calculated, since the ratio should be 50μg/ml plasmid DNA for 37,5μg/ml insert DNA.

Subsequently, reagents were added in the following order (reaction volume: 20 μl)

| Ligation reaction | |
|---|---|
| **Reagents** | **Volume** |
| (50μg/ml) DNA of pET-28a-bio | 4,16 μl |
| (37,5μg/ml) DNA of MetShaft61 | 3,13 μl |
| Sterile-distilled $H_2O$ | 9,17 μl |
| 10x T4 Ligase buffer | 2 μl |
| T4 Ligase | 1 μl |

(T4 ligase and T4 ligase buffer were purchased from New England Biolabs)

The reaction was conducted for 18 to 24 hours at 16°C.

## II. II. e. Competent cell preparation (for *E. coli* DH5α and BL21(DE3))

In order to yield transformed colonies, E. coli cells were prepared following a variation of the protocol described by Sambrook91. For the preparation of competent cells, 5ml of LB medium were inoculated with the desired strain and the cells were incubated overnight at 37°C. Then 50-100ml LB medium were inoculated with 0.5-1ml of the overnight cultures. The cells were incubated at 37°C while shaking at 250 rpm, until the optical density at λ=600 nm (O.D.600) was 0.4-0.6. The cultures were then centrifuged in falcon tubes at 2500 rpm for 10 min at 4°C. Cells were gently re-suspended in 15-30 ml TfbI buffer and cooled on ice for 30 min. The suspension was centrifuged again at 3500 rpm for 10 min at 4°C and the cells were resuspended gently in 2-4 ml TfbII buffer. Aliquots of 100μl were transferred to pre-cooled eppendorf tubes, frozen in liquid Nitrogen or dry ice and stored at -80°C.

| Buffer name | Components |
|---|---|
| TfbI buffer | 30mM $CH_3COOK$, 50mM $MnCl_2$, 100mM KCl, 10mM $CaCl_2$, 15% glycerol |
| TfbII buffer | 10mM MOPS pH:7, 75mM $CaCl_2$, 10mM KCl, 15% glycerol |

## II. II. f. Amplification and isolation of Bio-S plasmid

In order to confirm the successful cloning and insertion of gene into the plasmid as well as isolate and amplify this plasmid, competent cells DH5a *E. coli* cells were transformed with 10 μl of the ligation products. A small amount of cell solution was plated onto LB/agar plates with kanamycin and left to incubate at 37$^{o}$C for 20 hours. The produced colonies were inoculated overnight at 37$^{o}$C in 4ml LB with kanamycin. Plasmid isolation followed for 8 colonies with mini-preps. The successful cloning was verified by the digestion of the plasmid with the corresponding restriction endonucleases, by the appearance of not one but two bright bands at the expected kb in an 1% agarose gel, after electrophoresis.

## II. II. g. Heterologous over-expression of recombinant protein Bio-S in *Escherichia Coli*

❖ Transformation of competent E. coli BL21 (DE3) with Bio-S and birA plasmid DNAs

The first step in heterologous over-expression of Bio-S protein is the transformation of the cells by inserting both Bio-S protein and birA ligase plasmid DNAs, in susceptible E. coli BL21 (DE3) strain. A variation of the Sambrook described protocol was followed, where competent cells were transfected with plasmid DNA.

100μl of competent cells were taken out from -80$^{o}$C and placed in ice. After a few seconds, 1μl of both plasmid solutions was added and left for 30 minutes. The plasmid insertion was achieved by causing heat shock to the cells at 42$^{o}$C for 90 seconds, following their placement in ice for 2 minutes. After heat-shock, 700μl of LB medium was added and left to incubate at 37$^{o}$C for 1 hour, while shaking at 250 rpm. Subsequently, the suspension was centrifuged at 10k rpm for 1 min and most of the supernatant was removed. The pelleted cells were re-suspended in the remaining supernatant (about 100 μl) and plated onto a petri dish with LB and agar, containing 50 μg/ml kanamycin (for Bio-S plasmid DNA) and 34 μg/ml chloramphenicol (for birA plasmid DNA) as selection antibiotics, and left to incubate at 37$^{o}$C for 12-18 hours.

❖ Heterologous over-expression of recombinant Bio-S protein in E.Coli BL21.

The next step consisted in the cultivation of one transformed bacterial colony, with the over-expression of Bio-S following. A pre-culture was made by re-suspending one of the colonies in 5ml of LB medium with 50 μg/ml kanamycin and 34 μg/ml chloramphenicol and was incubated at 37°C for 5 hours, while shacked at 250 rpm.Subsequently, , the cell mixture was introduced to 50 ml LB medium (with kanamycin and chloramphenicol) and incubated at 37°C overnight, while shacked at 250 rpm. 1lt of LB medium was added in the culture (with kanamycin and chloramphenicol), and incubated at 37 °C, until the absorbance (O.D.) of the solution at 600nm was between 0,6 to 0,8. Protein expression from both plasmids started by adding 1mM of Isopropyl β-d-1-thiogalactopyranoside (IPTG) and biotinylation by subsequently adding 1,2 mg/ml biotin (in 10mM bicine solution, pH=8).

IPTG binds to lac repressor and inhibits its attachment to lac operon, resulting to the activation of the lac gene, which initiates the heterologous over-expression of Bio-S protein and BirA enzyme. By adding the biotin in the beginning of protein and ligase production, biotin is inserted in the bacterial cytoplasm and attaches to the lysine of the 16peptide sequence of the produced protein, by the produced ligase.

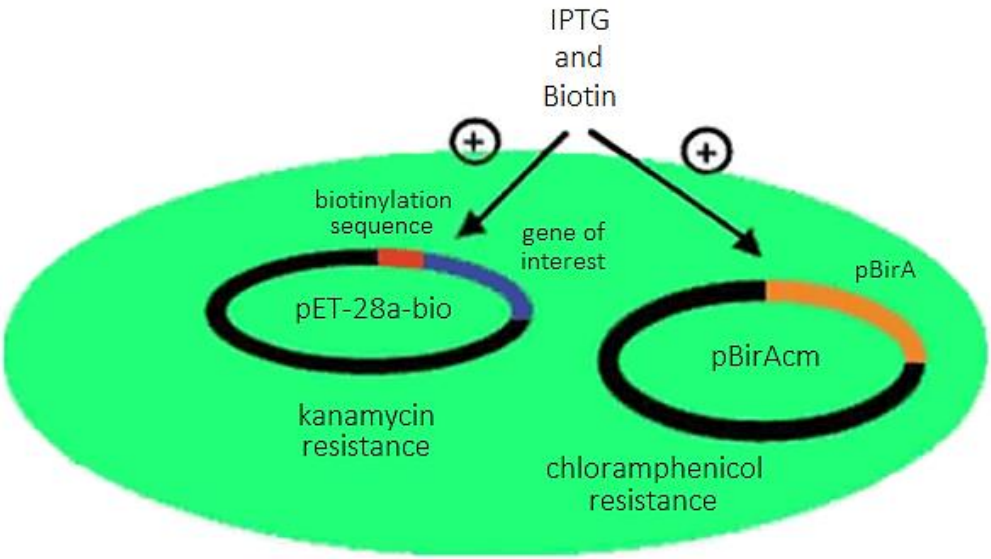


*Figure 11: Double IPTG induced plasmids in BL21 cells. The plasmid pBirAcm contains the gene of BirA biotin ligase (orange). pET-28a-bio contains the gene of the protein of interest to be biotinylated (blue) along with its biotinylation sequence (red)[45].*

The culture was left in the incubator at 37°C for 4 hours, where the overexpression's yield peaks. After 4 hours the cells were harvested by centrifugation at 7k rpm for 20 minutes at 4°C. The cell pellet was dissolved in 20ml of cell lysis buffer (20mM tris-HCl pH=9, 0,1M NaCl, 2% Triton, 2mg/ml lysozyme and 1x protein inhibitor solution) left for 30 minutes at 37°C and kept at -20°C for future use.

## II. II. h. Cell lysis and Bio-S purification by affinity chromatography

### ❖ Cell lysis

In order to collect and purify the overexpressed protein produced in the bacterial cytoplasm, a cell lysis procedure has to be followed. Cell lysis began with the degradation of cellular membrane by lysozyme in lysis buffer and by successively freezing the cell solution in liquid nitrogen to -195$^{o}$C and thawing it to a bath at 40$^{o}$C. The freeze-thaw process was repeated 3 times.

After that, the cell solution was placed in a French press, where a hydraulic cylindrical press forces the solution out of a narrow valve, resulting to high pressures of 1000 psi and the disruption of most cell membranes. After repeating this process twice, and in order to be sure that all cell membranes were broken, the solution was placed in an ice bath and was sonicated. The solution was sonicated for 30 seconds and left to cool for other 30 seconds, in order to prevent thermal degradation of the protein of interest. After cell lysis, 100μg/ml DNase I (Roche) and 100mM $MgSO_4$ was added to the solution to degrade DNA molecules.

### ❖ Collection and purification of Bio-S using Ni-NTA seeded sepharose beads

Due to the high yields and rapid expression of our protein, the protein tends to aggregate into big clusters of protein known as inclusion bodies, inside the bacterial cytoplasm. After cell lysis, in order to isolate and purify the protein in its native state, inclusion bodies should be washed and further dissociated .

In order to wash them, low concentrations of chaotropic agents and mild detergents are used successively to dissolve and easily remove most of the impurities. Initially, the cell lysed solution was centrifuged at 10krpm for 10 minutes at 4$^{o}$C, the pellet was reconstituted with 1M Urea and placed in circular shaking for 15 minutes. After another centrifugation at 10krpm for 10 minutes, the inclusion bodies were washed using the same method with 1% Triton followed by an additional washing with Tris-HCl buffer. After each washing, a sample from both solubilized pellet and supernatant was collected to ensure the successful washing.

The dissociation of the inclusion bodies is easily achieved by using high concentration of a strong chaotropic agent, such as magnesium chloride, guanidinium chloride, phenol or urea, that can disrupt inclusion body's stability and solubilize it. Such a process though demands the subsequent removal of the chaotropic agent in order to restore the native folding of the protein. After another centrifugation at 10krpm for 20minutes at 4$^{o}$C the pellet was reconstituted with urea buffer and solution was left stirring for 20 hours.

Affinity chromatography is a really efficient way to isolate and purify a certain protein from a protein mixture. NTA seeded sepharose beads can easily immobilize $Ni^{2+}$, which has high

affinity to poly-histidine sequences. Taking advantage of this affinity of poly-histidine sequence to cations of nickel, it is relatively easy to trap and isolate poly-his tagged proteins. The elution of the protein is achieved by introducing another molecule in the column with high affinity to $Ni^{2+}$, such as imidazole that acts as a competitor, and in high concentrations can displace/detach and therefore elute our protein.

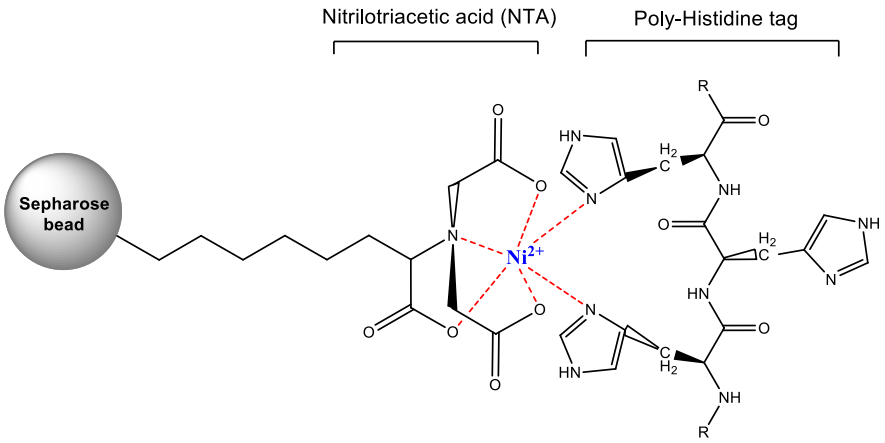


*Figure 12: Poly-histidine - Nickel - NTA complex attached to sepharose bead of affinity chromatography column.*

For the purification process *Ni Sepharose™ high performance* (GE Healthcare) was used and 2ml of this solution was placed in a chromatographic column and washed with distilled sterile $H_2O$ (5x the volume of chromatographic material), following a wash with 10ml urea buffer. Then, the cell lysed sample was added to the column and left to interact for 1 hour at 4°C in motion. Afterwards, the solution was left to pass through the column and the flow through was collected. The column was then washed twice with 2ml imidazole wash buffer, before starting the elution of the protein.

The elution phase started by adding twice 2ml imidazole elution buffer 50mM and collecting the elutions in different eppendorfs/falcons. Same process followed with imidazole elution buffers 100mM and 250mM. In every stage of washing and elution, samples of 50μl were collected. After that the column was washed successively with 2ml imidazole 1M, 10ml distilled $H_2O$ and 10ml 30% v/v aqueous ethanol solution.

| Buffer name | Components |
|---|---|
| Tris-HCl buffer | 20mM Tris-HCl pH=9 , 0,1M NaCl |
| Urea buffer | 20mM Tris-HCl pH=9 , 0,1M NaCl, 6M Urea |
| Lysis buffer | 20mM Tris-HCl pH=9, 0,1M NaCl, 2% Triton, 2mg/ml lysozyme and 1x protein inhibitor solution |
| Imidazole wash buffer | 20mM Tris-HCl pH=9 , 0,1M NaCl, 6M Urea, 5mM Imidazole |
| Imidazole elution buffer 50mM | 20mM Tris-HCl pH=9 , 0,1M NaCl, 6M Urea, 50mM Imidazole |
| Imidazole elution buffer 100mM | 20mM Tris-HCl pH=9 , 0,1M NaCl, 6M Urea, 100mM Imidazole |
| Imidazole elution buffer 250mM | 20mM Tris-HCl pH=9 , 0,1M NaCl, 6M Urea, 250mM Imidazole |

### II. II. i. Dialysis

As previously mentioned, after the purification and the collection of Bio-S, the presence of Urea keeps the protein in the denatured state, so, in order to allow it fold properly, removing of this solvent is mandatory. A quite efficient way to do that is by dialysis, where the protein solution is placed in a porous semi-permeable membrane, and submerged in a appropriate buffer. Solvent molecules can pass by through membrane pores by diffusion, resulting to significant reduction of molarity of the non-favorable/chaotropic solvent in protein solution and allowing the proper folding of the protein. Therefore, the protein solution was placed in a cellular dialysis membrane (molecular weight cutoff: 14kDa) and into 2lt of Tris-HCl buffer for 2 hours, while stirring. After that, the membrane with the protein solution was submerged once more to into 2lt of Tris-HCl buffer and left under stirring for 15-20 hours. The dialyzed solutions were concentrated using Amicon centrifugal filters (30 kDa cut-off) in order to achieve increase of protein concentration. After dialysis the samples were kept in room temperature to spontaneous self-assemble into amyloid fibrils for more than a week.

### II. II. j. Sodium Dodecyl Sulfate – Polyacrylamide Gel Electrophoresis (SDS-PAGE)

SDS-PAGE is a method used for the separation of proteins according to their molecular mass. In this study, this method was used to monitor the expression of the protein as well as its condition after each processing step (e.g. possible impurities, degradation products). In order to denature the protein boiling, SDS and β-mercaptoethanol are used. SDS binds to the linear protein molecules and confers a uniform negative charge. Then, the protein mixture is loaded on the SDS polyacrylamide gel and migrates across the gel in the presence of an electric field. The migration is size-dependent, where larger proteins migrate slower than smaller proteins, since they cannot fit easily into the pores of the gel.

In this study, the separating and stacking polyacrylamide gels were used with an acrylamide content of 7.5% and 4.5%, accordingly . The separating gels were prepared by mixing acrylamide with water and separating buffer. Polymerization was induced when APS and TEMED were added and the mixture was deposited between glass plates for electrophoresis. Isopropanol was added on top and the mixture was left to polymerize for approximately 1h. After gel polymerization, isopropanol was removed and the stacking gel mixture was deposited on top of the separating gel. Gel combs were placed on top of the stacking gel mixture for the formation of wells. The stacking gel was also left to polymerize for 30 min and the gel was transferred in the electrophoresis apparatus, which was filled with running buffer (1x).

The samples studied were mixed with loading buffer for SDS-PAGE, boiled for 5 min at 100 $^{o}$C and loaded in the wells. Protein molecular weight marker (Precision Plus Protein™ Dual Color Standards – BIORAD) was also loaded in a well and electrophoresis was performed at 200 V for about 1h. After their rinse with distilled water, the gels were stained with Coomassie Brilliant Blue R-250 stain, which binds to protein molecules. After destaining the gels, only the protein bands remained colored.

| Buffer name | Components |
|---|---|
| Lower Separating buffer | 187 g/l Tris-HCl pH:8.8, 0.4% w/v SDS |
| Upper Stacking buffer | 60.5 g/l Tris-HCl pH:6.8, 0.4% w/v SDS |
| 10x Running buffer | 30.3 g/l Tris, 144.1 g/l glycine, 10 g/l SDS |
| 3x SDS-PAGE Loading buffer (for 100ml stock) | 18.8 ml 1M Tris-HCl pH:6.8, 6 g SDS, 15 ml β-mercaptoethanol, 30 ml glycerol, a pinch of Bromophenol blue |
| Coomassie Brilliant Blue R-250 stain | 50% v/v methanol, 10% v/v acetic acid, 0,1% Coomassie Brilliant Blue |
| Destaining buffer | 10% v/v acetic acid 5% v/v methanol |

## II. II. k. Dot Blot for biotin detection

In a strip of a PVDF membrane, are blotted 10 μl of different concentrations of the recombinant protein Bio-S and 10 μl of 100 μg/ml of antibody – streptavidin alkaline phosphatase (from Streptomyces avidinii diluted 2000-fold) onto membrane as control. The membrane is incubated 1 hour at room temperature. The membrane and the spots should be dry before proceeding to the next step. The membrane is blocked with 5% dry milk in TTBS (50 mM Tris, 0.5 M NaCl, 0.05% Tween-20, pH:7.4) for 1 hour at room temperature. The blocking buffer is removed after this period but the membrane should be kept wet at all times for the remainder of the procedure. Incubation of the membrane with antibody – streptavidin alkaline phosphatase, followed, for 1hr at RT in TTBS. The membrane is then washed 3 times (10 minutes each) in TTBS on rocker followed by chemiluminescent detection with the 176μl/10ml of BCIP-NBT.

## II. II. l. Western Blot – Immuno-recognition

Western blot is a method that involves the immunological recognition of a protein using monoclonal antibodies. In the present study, monoclonal anti-His and anti-biotin antibodies were used. A Polyvinylidene fluoride (PVDF) membrane (Westran S - Whatman) was activated by submerging it in methanol. An electrophoresed polyacrylamide gel and the membrane were sandwiched between Whatman paper and sponges soaked in 1x Transfer buffer (18.8g/l glycine, 3 g Tris). All these were tightly packed and submerged in the transferring apparatus, which was filled with 1x Transfer buffer. An electrical field of 35 V was applied for about 2.5 h for the protein transfer onto the PVDF membrane.

The membrane was blocked by mild shaking in 5% w/v skimmed milk in 1x phosphate-buffered saline (PBS) for 1 hour at room temperature. After blocking, the PBS-milk was removed and the membrane was soaked in a solution of PBS-milk containing the primary antibody, mouse anti-His (Qiagen) or streptavidin alkaline phosphatase from Streptomyces avidinii diluted 2000-fold. The membrane remained in this solution overnight at 4$^{o}$C under mild shaking. The next day, the membrane was washed three times by shaking for 15 min in a solution of 1x PBS with 0.04% Tween 20. After washing again with PBS-milk, the membrane was soaked in a solution of PBS-milk containing the secondary antibody (anti-mouse IgG-alkaline phosphatase) diluted 20000-fold. The membrane remains in the solution of the secondary antibody for 2 h at room temperature under mild shaking. After the addition of the secondary antibody, the membrane was washed three times by shaking for 15 min in PBS-Tween 20 and then quickly washed with 1x alkaline phosphatase buffer. The protein bands detected by the antibodies were colored when 176μλ/10ml NBT-BCIP in 1x alkaline phosphatase buffer was added. Alkaline phosphatase dephosphorylates BCIP reacts with NBT to form an indigo-blue precipitate.

For biotin identification the antibody streptavidin alkaline phosphatase needs only 1h incubation in room temperature and subsequent washing with PBS-Tween 20 and 1x alkaline phosphatase buffer, followed by the NBT-BCIP color detection.

## II. II. m. Congo Red staining of Bio-S amyloid fibrils – birefringence

Congo Red staining, as mentioned before, is an optical technique, used for the verification of the presence of amyloid fibrils, where the Congo Red dye binds on amyloid fibrils and exhibits a apple green-yellow birefringence under polarized light.

A solution of 1mgr/ml Congo Red dye was prepared in 50% ethanol/water solution. Before the use, 0,01% v/v of 0,25M NaOH was added in the solution. For every 10μl of non-dense amyloid solution of Bio-S, 2μl of this solution was used. After 5 minutes the sample was placed on a glass coverslip for drying and for observation under optical microscope.

## II. II. n. Field Emission Scanning Electron Microscopy (FESEM)

Field Emission Scanning Electron Microscopy (FESEM) was used to observe Bio-S after its spontaneous self-assemble into amyloid fibrils in micro-scale level.

FESEM is a type of electron microscopy that scans the examined specimen with a very narrow high-energy focused electron beam. The signals of the interaction between this electron beam and the surface of the sample are gathered by a special detector, producing the sample's surface topography and, if needed, revealing its composition. This electron microscope provides a big range of magnifications and high resolution, while at the same time have a large depth of field that allows quite big focusing depth. Sample observation usually happens in high vacuum chambers and the samples have to be dry and electrically conductive. If not, the samples have to get dehydrated, fixed and sputter-coated with an electrically conductive material, such as gold or gold/palladium alloy.

After the deposition of 10 μl of the desirable sample concentration on glass coverslips, samples were left to air dry overnight. The next day, the samples were placed into the wells of a 36 well plate for the dehydration process. The samples were initially rinsed twice with double distilled $H_2O$. Then, in order to replace all water with ethanol and dehydrate the samples, successive rinses with 30%, 50%, 70%, 90%, 100% ethanol and 100% dry ethanol were followed for 7 minutes for each rinse. Samples then, are submerged in Bis(trimethylsilyl)amine (HMDS) overnight and left to air dry and kept in a glass desiccator.

One day prior observation, samples were sputter-coated with a 15 nm thick layer of gold. This was achieved by Physical Vapor Deposition (PVD) method where argon in plasma state is able to etch a gold target and catapult gold atoms onto the specimen and apply thin coatings of a single atom layer with extreme purity.

## II. II. o. Transmission Electron Microscopy (TEM)

Transmission Electron Microscopy (TEM) was used to observe Bio-S after its spontaneous self-assembly into amyloid fibrils in nano-scale level.

TEM is an electron microscopy where a narrow high-energy focused electron beam is transmitted through an ultrathin layer of a specimen. The signals of the interaction between this electron beam and the sample are gathered by a special detector beneath the sample, producing the sample's outline topography and interior if it is thin and hollow. This electron microscope provides big magnifications and captures high resolution and fine detail pictures, as TEM owns the smaller de Broglie wavelength of electrons. Sample observation happens in high vacuum chambers using special sample support meshes, called "grids".

A sample solution of 8μl was deposited onto a copper grid covered with carbon. The sample solution was left onto the grid for 2 min and the excess solution was removed using a filter paper. Subsequently, 8μl of 1% Uranyl acetate (for sample pH≤7) negative stain was applied, left for 3 min and the excess solution was removed using a filter paper.

## II. II. p. Functionalization with gold nanoparticles

Ni-NTA-Nanogold nanoparticle mixture was firstly sonicated for a few seconds. A sample of 0,1mg/ml of Bio-S amyloid fibrils in 20 mM Tris pH:8 and 150 mM NaCl was prepared. Gold nanoparticles solution in 10 times molar excess of amyloid fibrils was added to the Bio-S protein sample. The mixture was incubated for 30 minutes at 4°C. The solution was then centrifuged in Amicon centrifugal filters (30 kDa cut-off) to remove the unbound gold nanoparticles and the isolated labeled protein conjugates were re-suspended to the initial concentration.

For TEM observation, 8μl of this solution was loaded onto a carbon coated EM grid, left for 2 minutes and then was negatively stained with 8μl of 1% Uranyl acetate (for sample pH≤7) for 3 minutes. Control samples were also made of only Ni-NTA-Nanogold and only amyloid fibrils in the same way and concentration, for comparison.

# III. Results

## III. I. Cloning

### III. I. a. PCR Product

Following the PCR cloning the two samples (including MetShaft61 gene), the control sample and 2-log DNA ladder were loaded on a 1% w/v agarose gel for electrophoresis and the evaluation of the PCR product. The gel's red stain binds to the nucleic acid, gets excited by UV radiation and makes the samples visible to the naked eye.

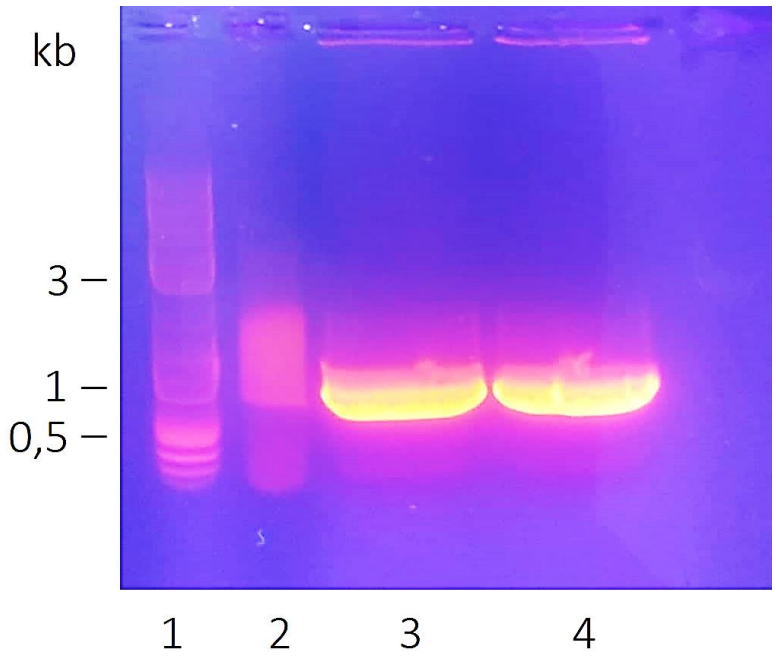


*Figure 13: Electrophorised PCR products on 1% w/v agarose gel*

Lanes: 1: Markers/DNA ladder + gel loading dye
2: control + gel loading dye
3: sample 1 + gel loading dye
4: sample 2 + gel loading dye

The PCR product of the 2 samples in lanes 3 and 4 are looking almost identical, presenting both a big band of nucleic acid close to the expected desirable length (theoretical MetShaft61 gene length: 999 bases). This ensures that MetShaft61 gene was successfully amplified in both samples. In the control sample, on the other hand, no distinguishable product seems to be amplified, confirming the specificity of the process.

III. I. b. Double digestion reaction - cut products

Double digestion with restriction enzymes XhoI and EcoRI (HF) on both the PCR product (MetShaft61 gene) and plasmid pET-28a-bio followed. The products were loaded on a 1% w/v agarose gel for electrophoresis for the evaluation of the reaction as well as the extraction of the clean DNA products.

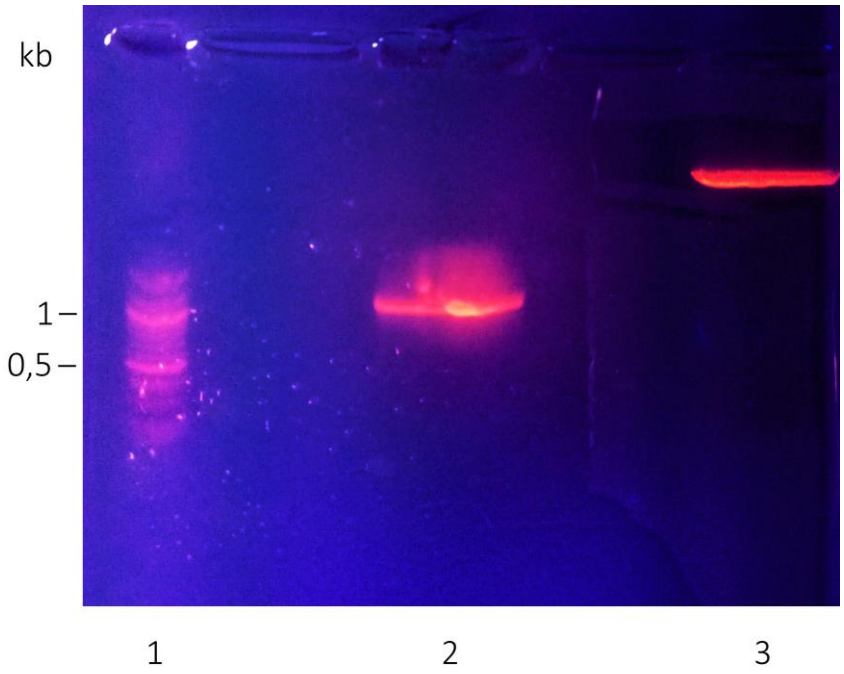


*Figure 14: Electrophorised PCR product and plasmid*

Lanes: 1: Marker/DNA ladder + gel loading dye
2: PCR product digested gene (MetShadt61 gene) + gel loading dye
3: plasmid pET-28a-bio digested gene + gel loading dye

The digested gene of PCR product (MetShadt61 gene) in lane 2 shows an almost distinct band close to 1k bases, close to the expected length (theoretical MetShaft61 gene length: 999 bases). The digested gene of plasmid pET-28a-bio in lane 3, appears as a very distinct solid band migrating quite higher compared to the PCR product, corresponding to the vector nucleic acid length. Unfortunately, the DNA ladder print is quite dim at this range of molecular mass and fails to disclose the exact length of the plasmid digested gene. Nevertheless, the band looks uniform and migrates in the expected length position , around 5k bases (pET-28a-bio plasmid : 5.4k bases).

III. I. c. Ligation products

After the extraction of both digested PCR product and Plasmid genes, ligation of the nucleic acids with T4 ligase followed. For amplification and isolation of the ligated plasmid, competent DH5a E. coli cells were transformed with the plasmid mixture and plated in a petri dish with LB/agar and kanamycin. Incubation of 8 of the produced colonies and extraction of the plasmids followed, using mini-preps. After digestion with the restriction enzymes, the gene samples were loaded in a 1% agarose gel for electrophoresis. Samples with double bands in their lanes would correspond to successfully ligated plasmids.

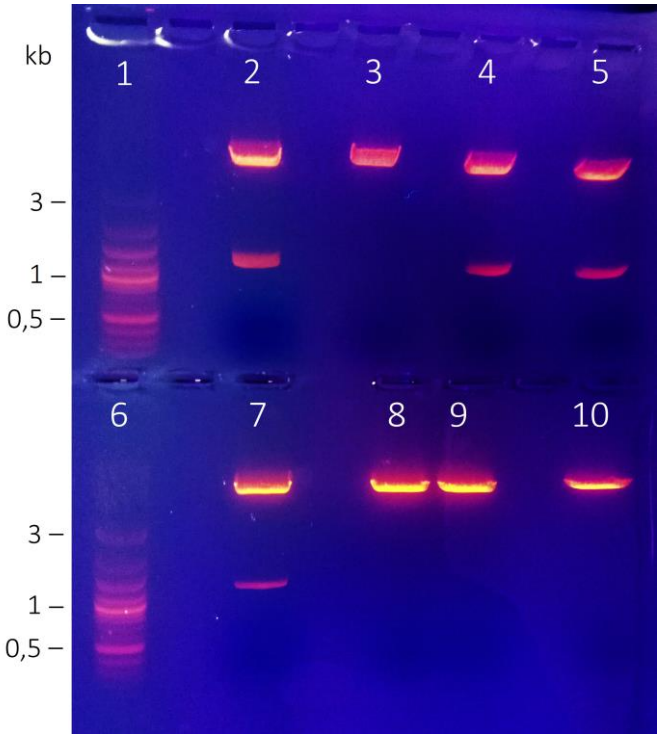


*Figure 15: Electrophoresed products after ligation on 1% w/v agarose gel*

Lanes: 1: Marker/DNA ladder + gel loading dye (GLD)
2: ligation product from colony No.1 + GLD
3: ligation product from colony No.2 + GLD
4: ligation product from colony No.3 + GLD
5: ligation product from colony No.4 + GLD
6: Marker/DNA ladder + GLD
7: ligation product from colony No.5 + GLD
8: ligation product from colony No.6 + GLD
9: ligation product from colony No.7 + GLD
10: ligation product from colony No.8 + GLD

Samples from colonies No. 2,6,7 and 8, corresponding to lanes 3,8,9 and 10 respectively, appear as only one band in their lanes, around 5k bases, indicating the presence of only the pET-28a-bio plasmid and thus, unsuccessful ligation and insertion of the desirable gene. On the other hand, ligated products from colonies No. 1,3,4 and 5, corresponding to lanes 2,4,5 and 7 respectively, appear as two bands; one around 5k bases, corresponding to the plasmid's gene and another one approximately to 1k bases, corresponding to the PCR product, indicating the successful ligation and insertion of the desirable gene.

## III. II. Over-expression products

### III. II. a. Bio-S production

When optical density of cell culture was approximately 0,6, a sample was taken and subsequently IPTG and biotin were introduced in the mixture and kept in the incubator at 37$^{o}$C for the over-expression of the protein. After 4 hours a sample was collected again and the cell culture was centrifuged for the isolation of cells. Those two samples were loaded on a 7,5% polyacrylamide gel for electrophoresis, in order to verify the successful over-expression and production of the Bio-S recombinant protein.

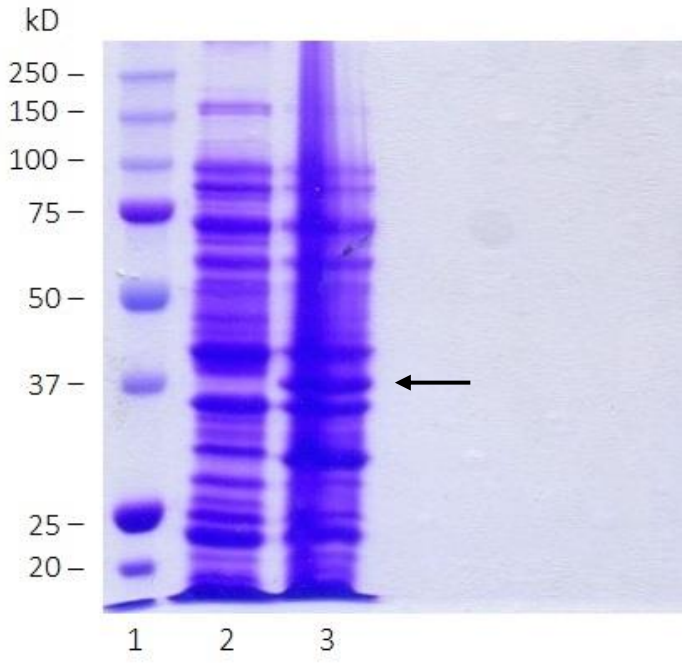


*Figure 16: Bacterial cell protein production before and after IPTG induction. Electrophoresis on a 7,5% polyacrylamide gel*

Lanes: 1: Marker
2: Before IPTG addition + SDS loading Buffer (SLB) / boiled
3: After 4 hours of IPTG induction + (SLB) / boiled

Lane 2 corresponds to the sample before IPTG addition and therefore no protein band is observed at the expected height. In the sample after 4 hours of incubation with IPTG, in lane 3, a band appears just around 37k Da that corresponds to Bio-S (Bio-S $M_w$:38,85882k Da), indicating the successful production of the recombinant protein. The band is indicated by an arrow.

III. II. b. Inclusion body washing

Before the dissociation of the inclusion bodies of Bio-S, inclusion bodies were washed successively with 1M Urea, 1% Triton and 20mM Tris-HCl buffer. After every centrifugation and reconstitution of inclusion body pellet, a sample was collected, mixed with SDS loading buffer and boiled for 5min. Samples were loaded on a 7,5% polyacrylamide gel for electrophoresis, in order to ascertain proper washing and removal of impurities.

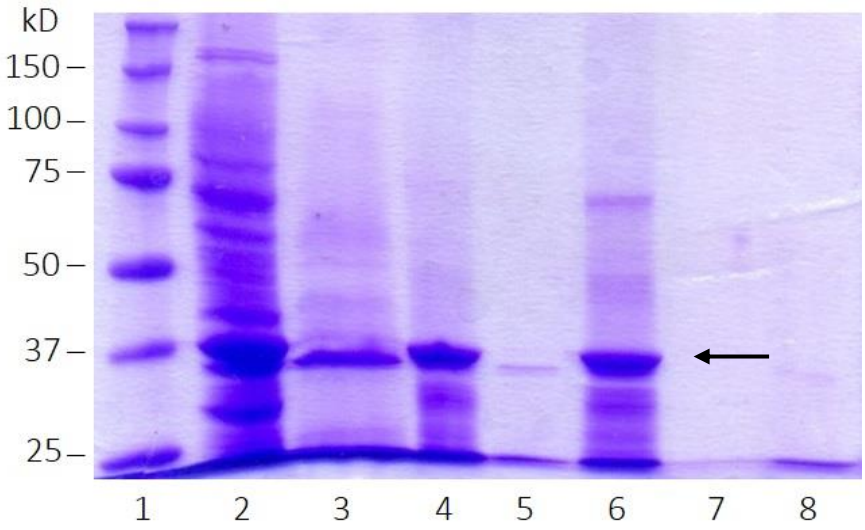


*Figure 17: Inclusion body washing samples after electrophoresis on 7,5% polyacrylamide gel*

Lanes: 1: Marker
2: Cell lysate + SDS loading buffer (SLB) / boiled
3: Supernatant after centr. + SLB / boiled
4: Cell pellet after Urea wash + SLB / boiled
5: Supernatant after Urea wash + SLB / boiled
6: Cell pellet after Triton + SLB / boiled
7: Supernatant after Triton wash + SLB / boiled
8: Supernatant after Tris-HCl buffer wash / boiled

The total mixture sample appearing in lane 2 shows the variety of bacterial proteins that result after cell lysis. In the same lane, around 37k Da two closely migrating bands appear, one corresponding to Bio-S and another one corresponding to an outer membrane protein (assuming porin omp A, appears around 36k Da). Supernatant samples of each washing corresponding to lanes 3,5,7 and 8 are indicating the proteins removed from the pellet after every washing and centrifugation, including most of the outer membrane protein near Bio-S. The protein pellet sample in lane 6 indicates significant purification compared to the cell lysate (lane 2).

III. II. c. Protein purification

After the inclusion body dissociation with 6M Urea, the protein solution was loaded to a Ni seeded NTA-sepharose column, left to interact and then washed twice. Elution of Bio-S protein was induced by introducing imidazole solutions of 50mM, 100mM and 250mM in the column and collecting the flow-through. Samples of collected elutions were mixed with SDS loading buffer, boiled and loaded on a 7,5% polyacrylamide gel for electrophoresis, for confirmation of successful purification.

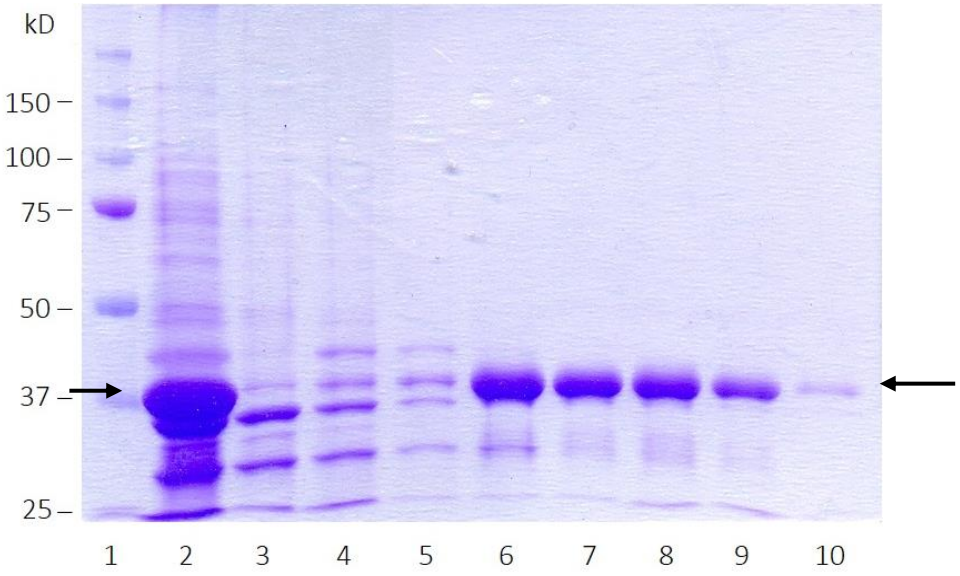


*Figure 18: Electrophorised samples of purification process on 7,5% polyacrylamide gel*

Lanes: 1: Marker
2: Cell lysate(Urea) + SLB / boiled
3: Flow-through + SLB / boiled
4: Wash 1 + SLB / boiled
5: Wash 2 + SLB / boiled
6: $E_1$ 50mM Imidazole + SLB / boiled
7: $E_2$ 50mM Imidazole + SLB / boiled
8: $E_3$ 100mM Imidazole + SLB / boiled
9: $E_4$ 100mM Imidazole + SLB / boiled
10: $E_5$ 250mM Imidazole + SLB / boiled

The sample before purification, appearing in lane 2, shows the presence of many proteins in the mixture. In the same lane, around 37kDa two bands appear again, where one represents Bio-S (Bio-S $M_w$:38,85882 kDa). After the solution interacts with the column, flow-through sample in lane 3 shows the removal of some proteins, as with the two sequential washes corresponding in lanes 4 and 5. Lanes 6 and 7 correspond to two elutions of Bio-S protein with 50mM Imidazole, where most of the protein seems to be eluted. Lanes 8, 9 and 10 show the decreasing subsequent elution of the protein by two washes with 100mM and 1 with 250mM Imidazole. Collected protein seems to be significantly purified.

## III. III. Dot Blot for biotin detection

Small amounts of different concentrations of Bio-S were placed on forms of dots on a PVDF membrane, as well as a dot of antibody to streptavidin conjugated with alkaline phosphatase for positive control. The same antibody was introduced on the membrane, under proper conditions, followed by the addition of NBT-BCIP in order to stain and verify the eventual biotin attachment.

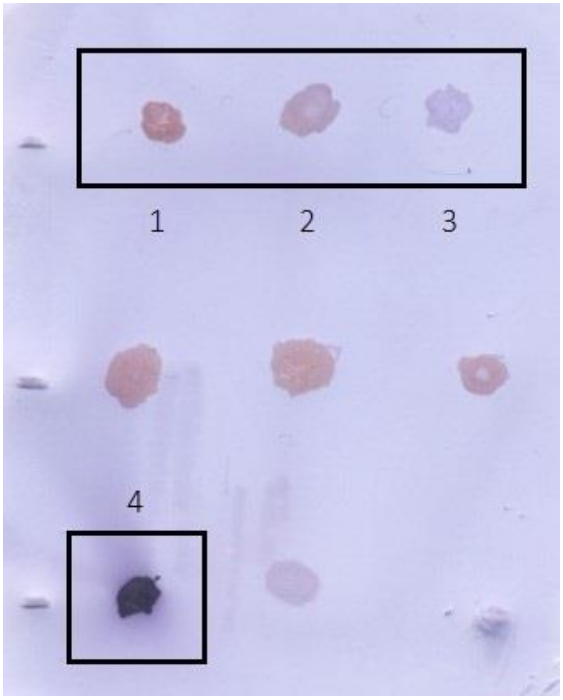


*Figure 19: Immunostaining of different concentrations of Bio-S on PVDF membrane for biotin detection*

Dots: 1: 0,2mg/ml Bio-S
2: 0,5mg/ml Bio-S
3: 1mg/ml Bio- S
4: 100mg/ml streptavidin alkaline phosphatase (antibody) – positive control

Staining of plain antibody streptavidin alkaline corresponding to dot No. 4 shows that the darker and "bluer" the dot is, the more antibody was bound to the biotinylated protein. Gradual increase of Bio-S concentrations corresponding to dots No. 1, 2 and 3 accordingly, shows the gradual shifting from beige to blue, indicating the increase of antibody attachment and thus, increase of biotin content. This result conforms the biotin attachment to Bio-S protein as well as the direct correlation of Bio-S concentration to biotin concentration attached.

## III. IV. Immunological recognition through western blot

Figure 20 shows a Western blot of an electrophoresed polyacrylamide gel of Bio-S sample, where the purified protein was transferred onto a PVDF membrane. Primary and secondary (when required ) antibody-phosphatases were introduced to the membranes, under proper conditions, followed by the addition of NBT-BCIP in order to stain and verify the presence of histidine tag and biotin attachment.

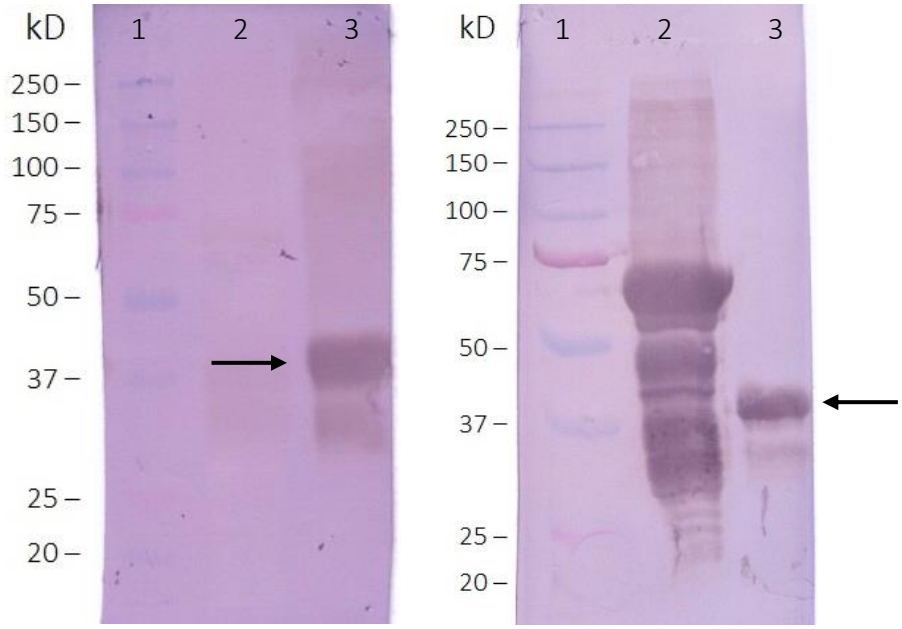


*Figure 20: Immunostaining of Bio-S on PVDF membranes for biotin (left) and his-tag (right) detection*

Lanes: 1: Marker
2: Test of another protein (ignore)
3: Bio-S + strept. Alk-pho/tase

1: Marker
2: Test of another protein (ignore)
3: Bio-S + mouse anti-his + anti-mouse Alk-pho/tase

In both biotin and his-tag detection blots , a distinct protein band appears just above 37k Da, corresponding to the detection of both in Bio-S (Bio-S $M_w$:38,85 kDa), confirming the successful and proper production of the recombinant protein with the additional functionalities. Another faint band is noticeable, below 37k Da in both cases, attributed to a degradation product of the protein from its C terminus.

## III. V. Congo red stained amyloid fibrils of Bio-S

Purified Bio-S was left for more than a week in room temperature to form amyloid fibrils, following dialysis. Congo Red solution was prepared by adding to it NaOH, and then mixed with 1mg/ml of Bio-S protein. After deposition and drying on a glass coverslip, the sample was observed under an opticalstereoscope. Observation under crossed polarizers can unveil the characteristic birefringence that amyloid fibrils exhibit once dyed by Congo Red, and verify their formation.

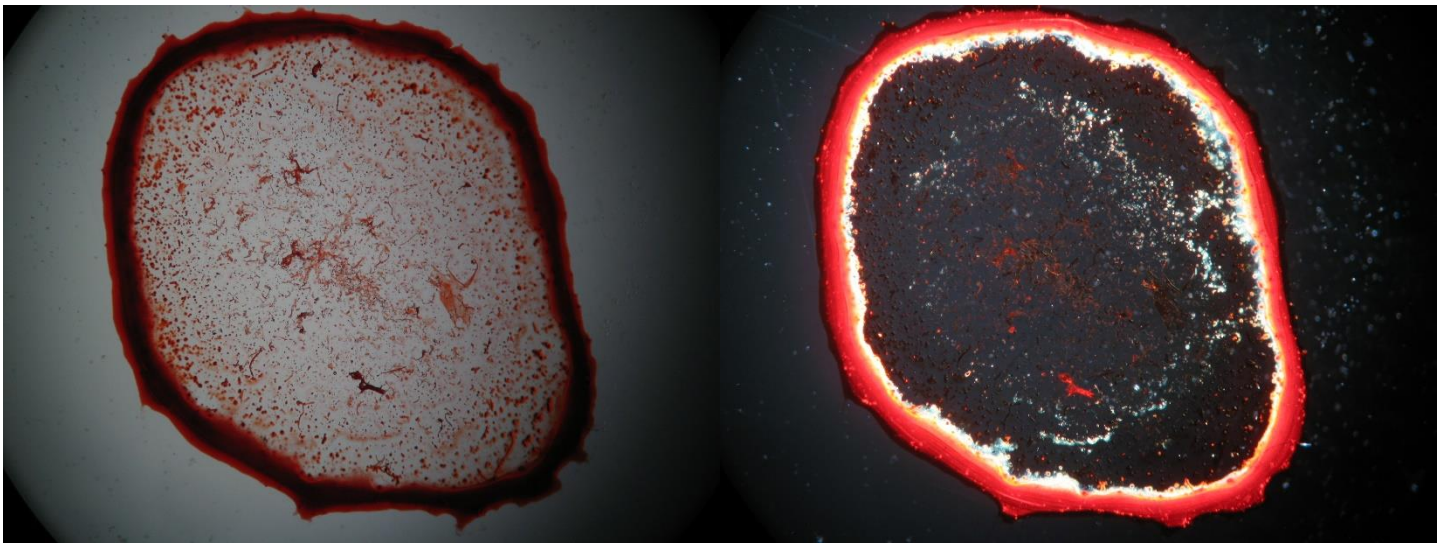

*Figure 21: Congo red stained amyloid fibrils of Bio-S under white (left) and polarized light (right)*

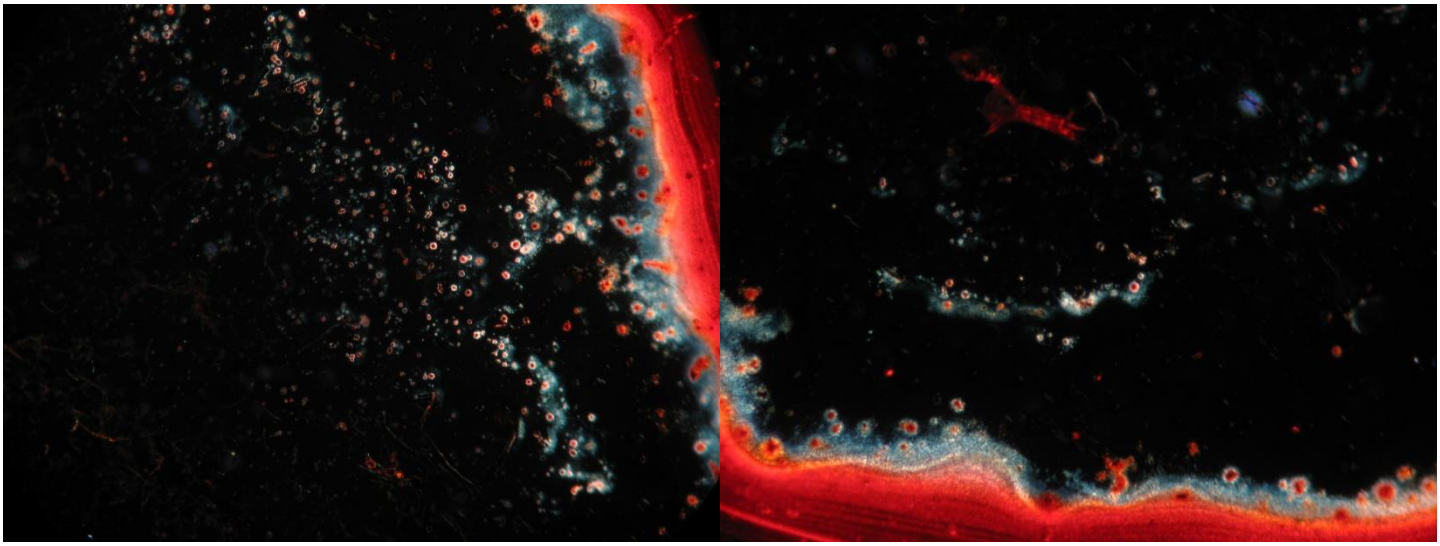

*Figure 22: Birefringence of Congo Red stained amyloid fibrils of Bio-S after exposure to polarized light*

Comparison of the images with and without polarizer can clearly show the cyan-yellow birefringence of the amyloid fibrils. Cyan-yellow colors can be, also, easily seen after magnification in different positions in the sample, indicating the presence and formation of amyloid fibrils.

## III. VI. FESEM images – Conformation verification of amyloid fibril formation

### III. VI. a. Dehydrated amyloid fibrils of Bio-S

Samples of 1mg/ml of amyloid fibrils were deposited on glass coverslips and got dehydrated using ethanol and HMDS. Coating of 15nm thick layer of Au was deposited on every specimen using PVD sputtering method to make it conductive, in order to be observed in FESEM.

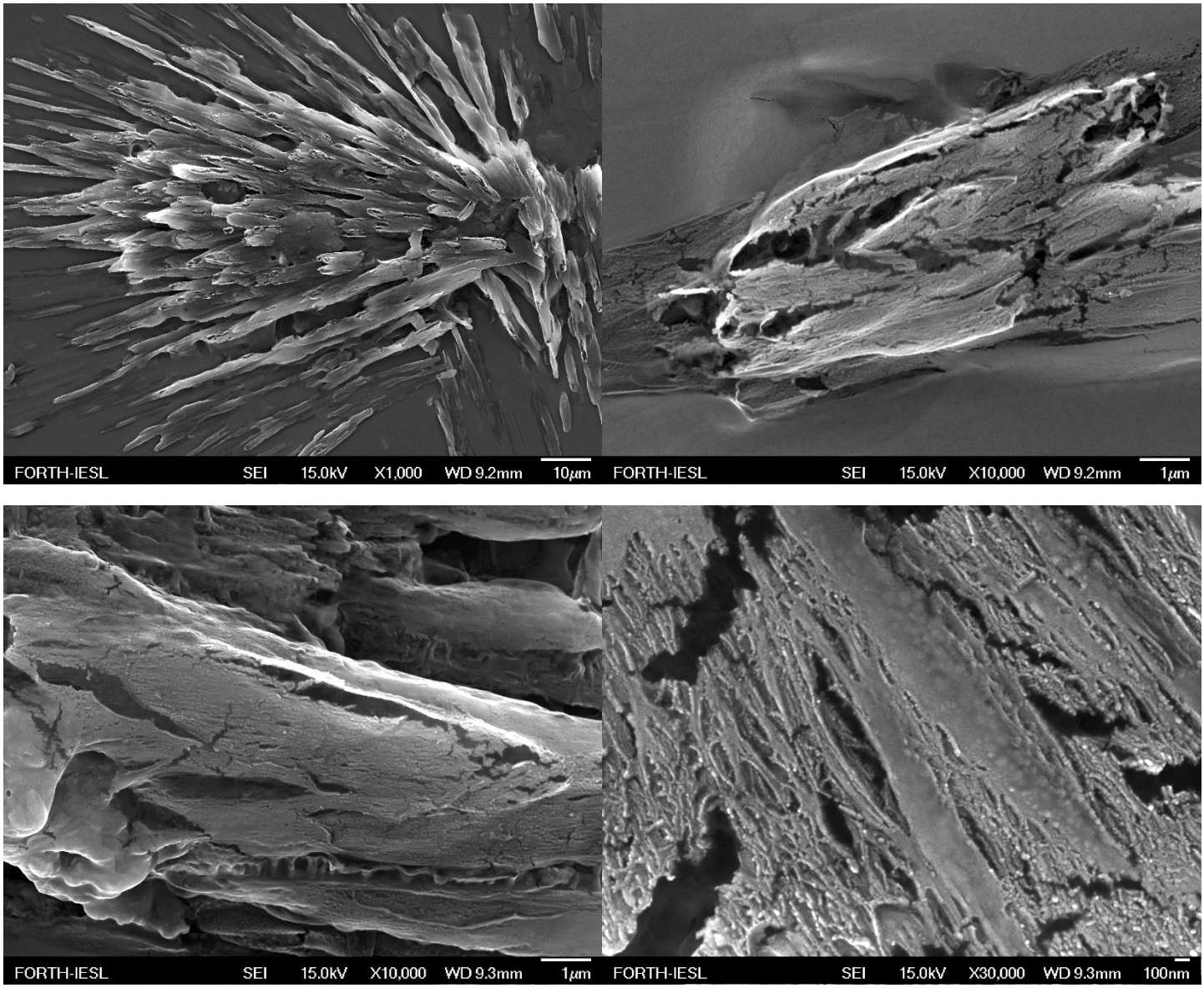


*Figure 23: FESEM images of conformation of Bio-S amyloid fibrils (1mg/ml) after HMDS dehydration*

Amyloid fibrils of Bio-S seem to aggregate into big solenoid crystal like structures with smooth surfaces that in first glance do not resemble to the typical fibril like images. By magnifying close to the surface of these structures, bloating and cracking of the surface was

observed, due to the high energy electron beam radiation. These structures consist of small individual fibrils that tightly entangle with each other in an unoriented conformation. This happens during the dehydration process, which abruptly evaporates any trapped water molecules, shrinking and gluing these small fibrils together, resulting into this homogenous "nanosheet" formation.

### III. VI. b. Air dried amyloid fibrils of Bio-S

The same experiment was repeated after several weeks with samples of 1mg/ml of amyloid fibrils deposited on glass coverslips that left to dry in a glass desiccator for several days. Again, 15nm thick layer of Au was deposited on every specimen using the PVD sputtering method, in order to be observed in FESEM.

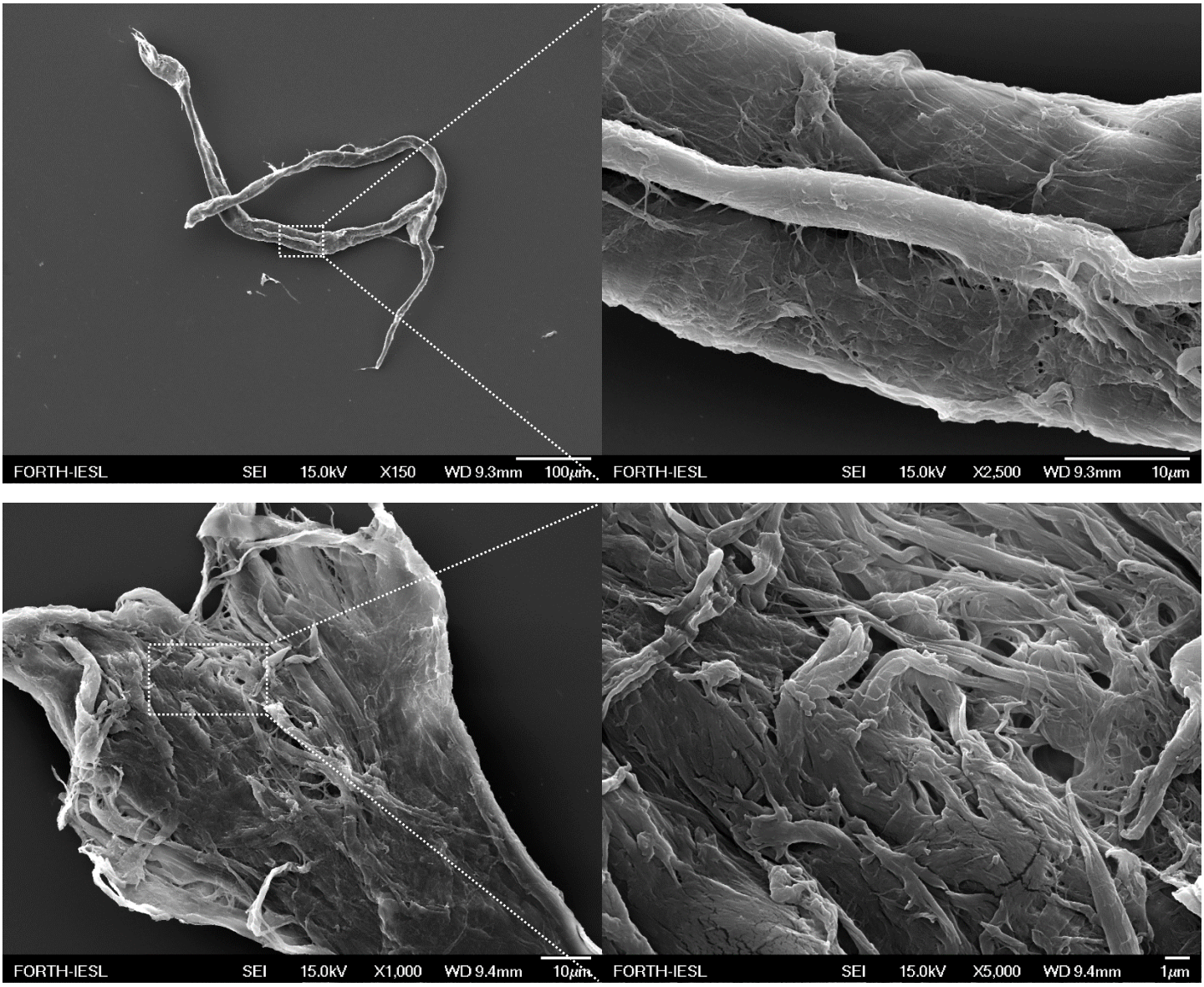


*Figure 24: FESEM images of conformation of air dried mature Bio-S amyloid fibrils (1mg/ml) and their magnifications*

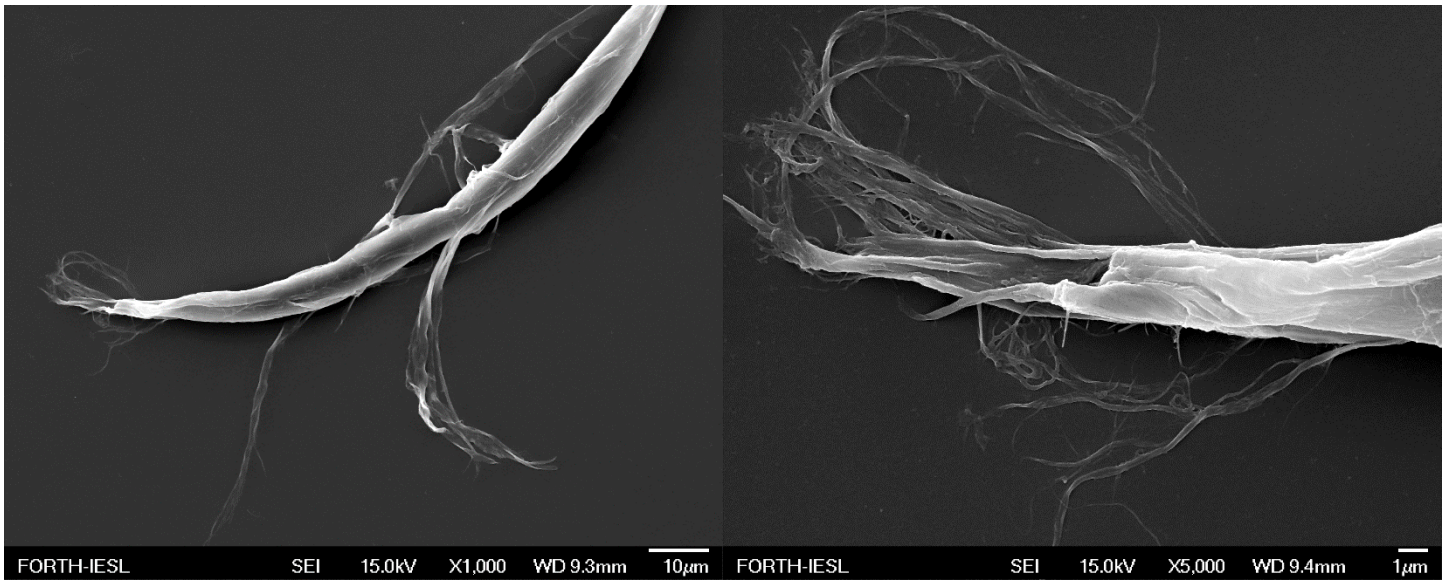


*Figure 25: FESEM images of conformation of air dried mature Bio-S amyloid fibrils (1mg/ml)*

Mature air dried amyloid fibrils of Bio-S protein seem to aggregate and form long, thread-like structures. Sometimes these creating long-range conformations, occasionally reaching the scale of millimeters. At first sight the magnitude and shape of these structures do not remind the usual "randomly oriented" image of amyloid fibrils. Tight and complex entanglement of smaller individual fibrils makes these structures look uniform with smooth surface. However, magnifying the surface of these structures unveils the formation and complexity of individual smaller fibrils.

The difference between those two conformations can be attributed mostly to the conditions under which the drying process was carried out, firstly with successive rinses with ethanol and then HMDS submersion for dehydration. Another factor contributing to this difference could be the time period amyloid fibrils were left to mature.

## III. VII. Transmission electron microscopy images

### III. VII. a. Amyloid fibrils of Bio-S

Samples of 8µl of 0,1mg/ml Bio-S amyloid fibrils were deposited onto a carbon covered copper grid for 2 min with excess removed and negatively stained with 1% Uranyl acetate in the same way for 3 min. After several days of air drying the samples were observed by TEM.

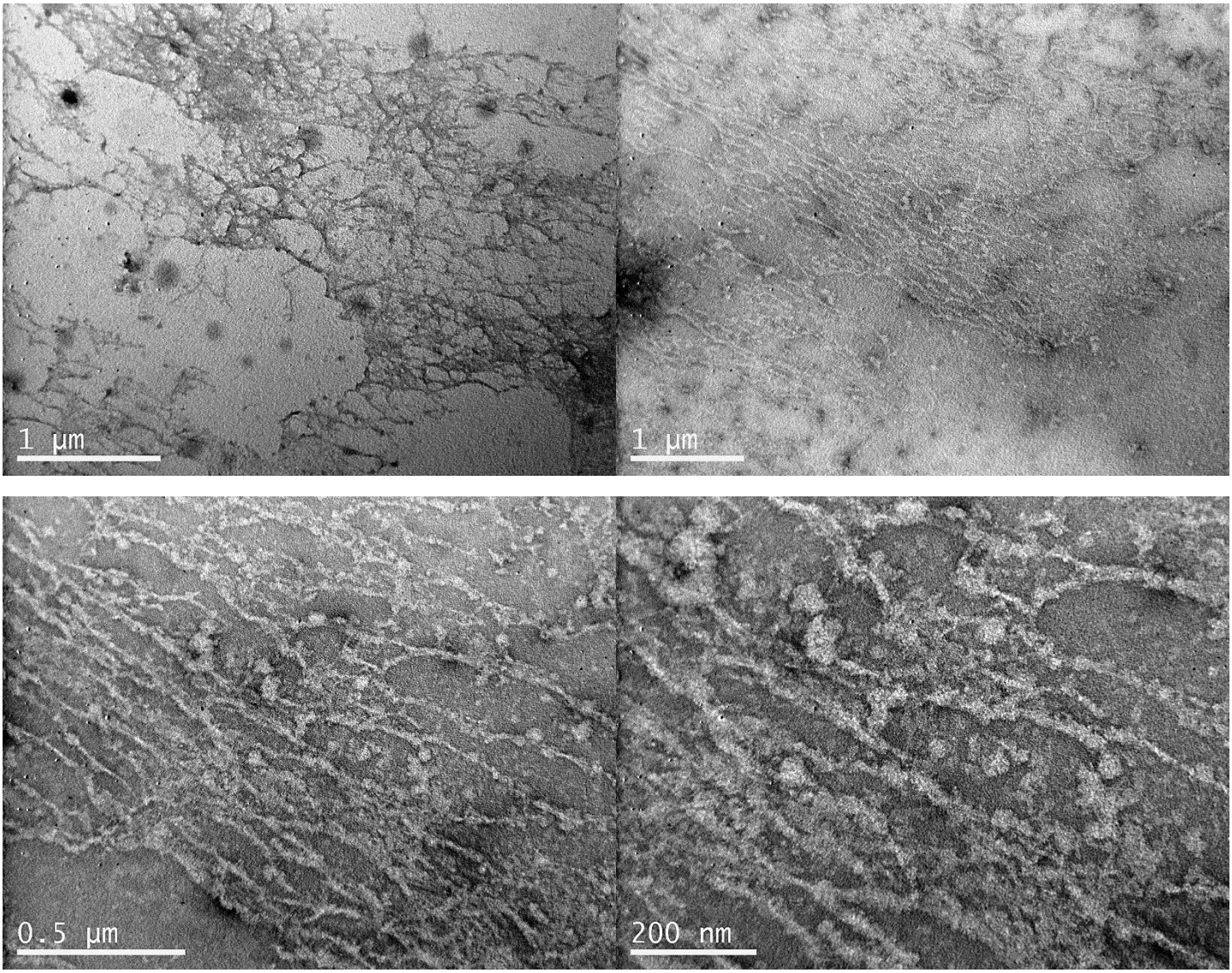


*Figure 26: TEM images of conformation of mature Bio-S amyloid fibrils (0,1mg/ml) on micro and nano-scale*

Mature amyloid fibrils of Bio-S can be easily observed using TEM. Fibrils under TEM observation appear to have the typical fibril like conformation. They seem to be highly packed and entangled in some areas and demonstrate collective direction in other areas.

III. VII. b. Bio-S amyloid fibrils functionalized with Ni-NTA-Nanogold

Bio-S amyloid fibrils were incubated with Ni-NTA-Au nanoparticle solution while the unbound excess was removed with amicon filter centrifugation. Samples of 0,1mg/ml functionalized Bio-S were deposited onto a carbon covered copper grid for 2 min with the excess of the sample being removed and then further negatively stained with 1% Uranyl acetate in the same way for 3 min. Samples were observed after several days by TEM.

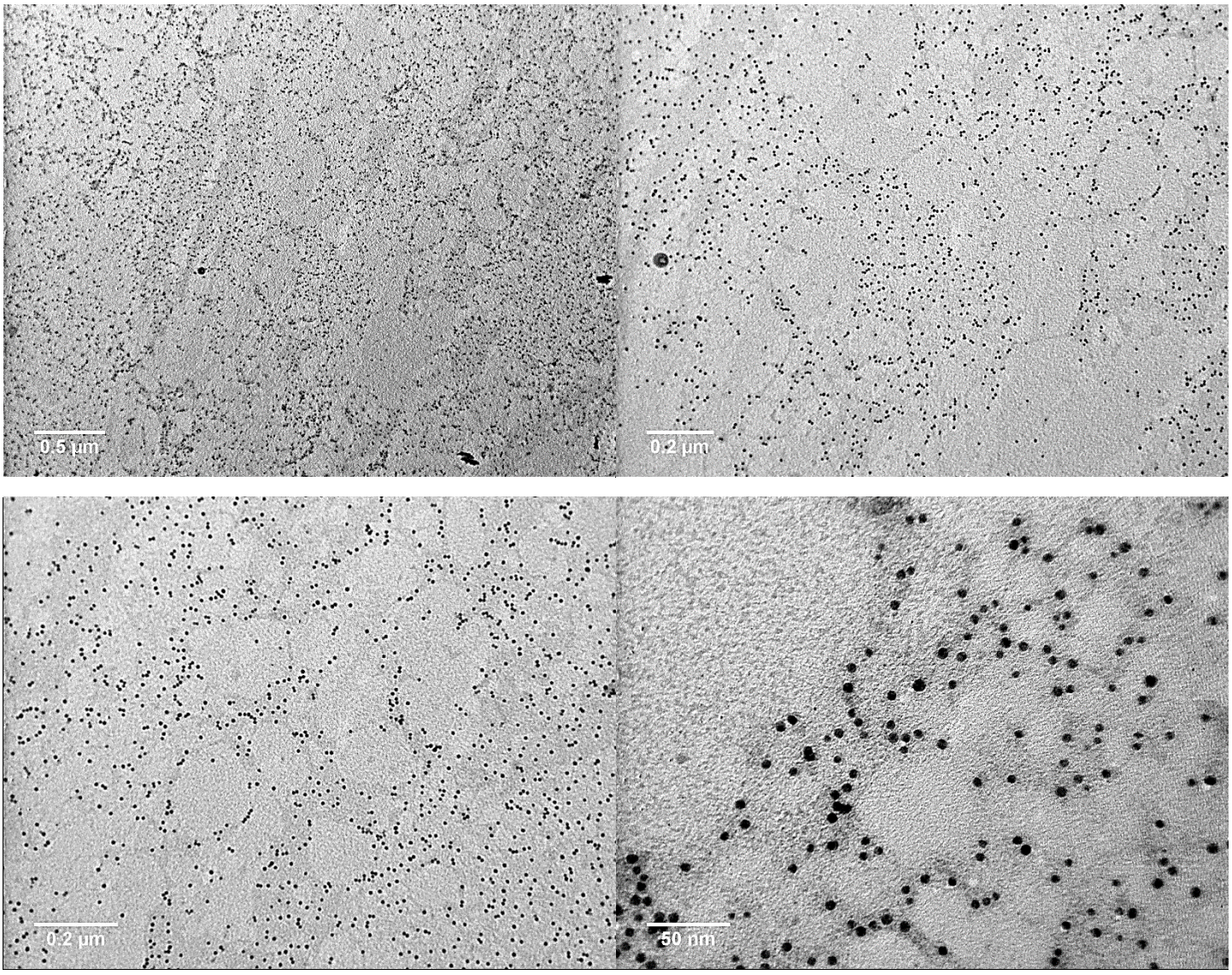


*Figure 27: TEM images of conformation of Bio-S amyloid fibrils (0,1mg/ml) functionalized with Ni-NTA-Au nanoparticles*

The abundant presence of Au nanoparticles (small black dots) coinciding with the Bio-S amyloid fibrils verifies their successful attachment on the protein. Magnifications on the specimen show un-even disperse of gold nanoparticles on their surface, indicating specific attachment of the nanoparticles on the amyloid fibrils through the histidine tag.

III. VII. c. Ni-NTA-Gold nanoparticles

Ni-NTA-Gold nanoparticles corresponding to the amount used to functionalized 0,1mg/ml Bio-S amyloid fibrils were deposited onto a carbon covered copper grid for 2 min with excess removed and left to air dry for several days before observed by TEM.

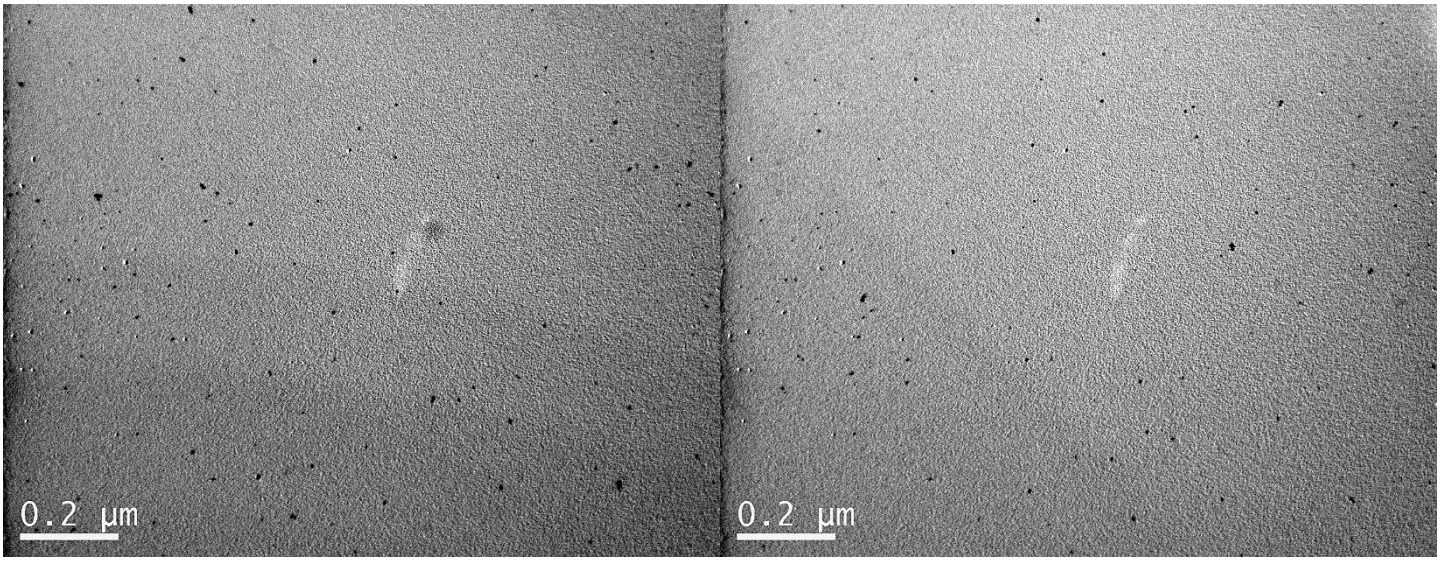


*Figure 28: TEM images of unbound Ni-NTA-Au nanoparticles*

Gold nanoparticles show to be evenly dispersed everywhere on the grid, indicating random distribution on it. This verifies the specific attachment of Ni-NTA-Au nanoparticles on the Bio-S amyloid fibrils and their successful functionalization.

# IV. Conclusions

The present work aimed at the design, production and characterization of a new recombinant protein, named Bio-S, towards its development as a multifunctional scaffold suitable for biological applications. The design of this protein was based on an already well studied protein MetShaft61, inspired from the fiber of Adenovirus type 2, that can produce stable amyloid fibrils. Taking advantage of this ability, in combination with the introduction of a histidine tag and a biotin binding sequences in its construct, Bio-S can form amyloid fibrils able to be functionalized with a wide range of desirable decorations on their surface.

The expression and production of this protein's gene was successfully achieved by inserting the PCR amplified gene of MetShaft61 in pET-28a-bio plasmid. Transformation with the ligated plasmid and BirA plasmid of *E. coli* cells, their proper incubation with the subsequent induction with IPTG, by the presence of biotin, and their lysis, resulted to the heterologous overexpression and production of Bio-S.

Due to the abundant overexpression rate and aggregating nature of the construct, the expressed protein is stored within the bacterial inclusion bodies. Washing of proteins' inclusion bodies and their subsequent dissociation was achieved by introducing them to Urea solutions with different concentrations. Protein isolation and purification was completed through successive washing and elution using affinity chromatographic material, based on his-tag's affinity to $Ni^{2+}$. Amyloid fibril formation was favored after removing the denaturing agent (urea) from the protein solution through dialysis.

The presence of Biotin and histidine tag was verified through the methods of dot blot and western blot, where immuno-staining recognition confirmed their presence. Amyloid fibril formation was firstly indicated by the birefringence that the protein solution exhibited following staining with Congo Red. FESEM observation of Bio-S confirmed the presence of long fibril conformations of tightly packed and highly entangled individual amyloid fibrils of the protein. Moreover, the formation of "nanosheet" conformations was also suggested from the FESEM images. Images of amyloid fibrils of Bio-S observed under TEM microscopy sheds light to the arrangement and details of conformation of these structures.

Comparison of functionalized amyloid fibrils with Au nanoparticles to non-functionalized and plain/pure Au nanoparticles, proved the successful specific attachment of Au nanoparticles on amyloid fibrils and therefore their functionalization.

# V. Future work

Future work of this project would aim to form proper scaffold structures out of Bio-S amyloid fibrils, from methods like freeze-drying or electrospinning. Cell cultivation on these scaffolds and checking of their biocompatibility through tests of cell viability should also be examined. More characterization experiments like mechanical and chemical characterization of the amyloid fibrils should also be conducted for the better understanding of the limitations of the use of this material.

Furthermore, functionalization with more diverse decorations can allow the use of Bio-S amyloid fibrils to a wide range of possible applications. Such applications includes development of biocompatible scaffold that carries therapeutical proteins, drugs signaling molecules on its surface through biotin, streptavidin or his-tag conjugation. Other possible applications include engineering of metal binding scaffolds or the attachment of growth factors towards the development of fibrillar nanosheet scaffolds that can trigger and/or regulate specific cell responses.

# VI. References


[1]. Text of the Convention on Biological Diversity (CBD), Use of terms

[2]. Verma A. S., Agrahari S., Rastogi S., Singh A., Biotechnology in the Realm of History, *J Pharm Bioallied Sci.* 2011 Jul-Sep; 3(3): 321–323

[3]. Langer R., Vacanti JP., Tissue engineering. *Science*. **260** (5110): 920–6, May 1993. *Bibcode:1993Sci.260..920L*. *doi:10.1126/science.8493529*. *PMID 8493529*

[4]. Bergmann C., Stumpf A. Dental Ceramics: Microstructure, Properties and Degradation *Springer Berlin Heidelberg*, 2013 https://doi.org/10.1007/978-3-642-38224-6

[5]. Dzobo K., Thomford N. E., Senthebane D. A., et al. Advances in Regenerative Medicine and Tissue Engineering: Innovation and Transformation of Medicine. *Stem Cells Int*. 2018;2018:2495848. Published 2018 Jul 30. doi:10.1155/2018/2495848

[6]. Ma P. X., Biomimetic materials for tissue engineering. *Adv Drug Deliv Rev*. 2008;60(2):184–198. doi:10.1016/j.addr.2007.08.041

[7]. Subhadeep D., Reeba S. J., Komal P., Namrata S., Samir K. M., Amyloid Fibrils: Versatile Biomaterials for Cell Adhesion and Tissue Engineering Applications, *Biomacromolecules* 2018 19 (6), 1826-1839, DOI: 10.1021/acs.biomac.8b00279

[8]. Chiti F., Dobson C. M., Protein Misfolding, Amyloid Formation, and Human Disease: A Summary of Progress Over the Last Decade, *Annual Review of Biochemistry,* 2017 86:1, 27-68

[9]. Chiang P. K., Lam M. A., Luo Y., The many faces of amyloid beta in Alzheimer's disease, *Current Molecular Medicine,* September 2008. 8 (6): 580–4. doi:10.2174/156652408785747951. PMID 18781964.

[10]. Irvine G. B., El-Agnaf O. M., Shankar G. M., Walsh D. M., Protein aggregation in the brain: the molecular basis for Alzheimer's and Parkinson's diseases. *Molecular Medicine*,2008, 14 (7–8): 451–64. doi:10.2119/2007-00100.

[11]. Haataja L., Gurlo T., Huang C. J., Butler P. C., Islet amyloid in type 2 diabetes, and the toxic oligomer hypothesis. *Endocrine Reviews*, May 2008, **29** (3): 303–16. doi:10.1210/er.2007-0037.

[12]. Dueholm M. S., Albertsen M., Otzen D., Nielsen P. H., Webber M. A. (ed.), Curli functional amyloid systems are phylogenetically widespread and display large diversity in operon and protein structure. *PLOS ONE*, 2012, **7** (12): e51274, Bibcode:2012PLoSO...751274D doi:10.1371/journal.pone.0051274.

[13]. Fowler D. M., Koulov A. V., Alory-Jost C., Marks M. S., Balch W. E., Kelly J. W., Functional amyloid formation within mammalian tissue. *PLoS Biology*, 2006, **4** (1): e6, doi:10.1371/journal.pbio.0040006.

[14]. Fowler D. M., Koulov A. V., Balch W. E., Kelly J. W., Functional amyloid - from bacteria to humans., *Trends in Biochemical Sciences*, 2007, **32** (5): 217–24. doi:10.1016/j.tibs.2007.03.003.

[15]. Toyama B. H., Weissman J. S., Amyloid structure: conformational diversity and consequences, *Annual Review of Biochemistry*, 2011, ***80****: 557–85.* doi:10.1146/annurev-biochem-090908-120656.

[16]. Cao Y., Mezzenga R., Food protein amyloid fibrils: Origin, structure, formation, characterization, applications and health implications., *Advances Colloid Interface Sci*., 2019, Jul;269:334-356. doi: 10.1016/j.cis.2019.05.002.

[17]. Moretti M., Proietti Zaccaria R., Descrovi E. *et al.,* Reflection-mode TERS on Insulin Amyloid Fibrils with Top-Visual AFM Probes. *Plasmonics* **8,** 25–33 (2013). https://doi.org/10.1007/s11468-012-9385-x

[18]. Nesterov E. E., Skoch J., Hyman B. T., Klunk W. E., Bacskai B. J., Swager T. M., In vivo optical imaging of amyloid aggregates in brain: design of fluorescent markers., *Angewandte Chemie*, 2005, **44** (34): 5452–6. doi:10.1002/anie.200500845.

[19]. Eisenberg D., Jucker M., The amyloid state of proteins in human diseases. *Cell*. 2012 ;148(6):1188–1203. doi:10.1016/j.cell.2012.02.022.

[20]. Tanskanen M., Feng D. (ed), Amyloid — Historical Aspects *Open access peer-reviewed Edited Volume, IntechOpen,* 2013, DOI: 10.5772/53423

[21]. J. D. Bronzino, *"The Biomedical Engineering Handbook, Second Edition"*, 2000, Section 4

[22]. Deidda G., Jonnalagadda S. V. R., Spies J. W., Ranella A., Mossou E., Forsyth V. T., Mitchell E. P., Bowler M. W., Tamamis P., Mitraki A., Self-Assembled Amyloid Peptides with Arg-Gly-Asp (RGD) Motifs As Scaffolds for Tissue Engineering. *Acs Biomaterials Science & Engineering,* 2017, 3 (7), 1404-1416. DOI: 10.1021/acsbiomaterials.6600570.

[23]. Holmes T. C., de Lacalle S., Su X., Liu G., Rich A., Zhang S., Extensive neurite outgrowth and active synapse formation on self-assembling peptide scaffolds. *P. Natl. Acad. Sci.* 2000, *97* (12), 6728. DOI: 10.1073/pnas.97.12.6728.

[24]. Ellis-Behnke R. G., Schneider G. E., Peptide amphiphiles and porous biodegradable scaffolds for tissue regeneration in the brain and spinal cord. *Methods in molecular biology* 2011, *726*, 259-81. DOI: 10.1007/978-1-61779-052-2_17.

[25]. Kokotidou C., Jonnalagadda S. V. R., Orr A. A., Vrentzos G., Kretsovali A., Tamamis P., Mitraki A., Designer Amyloid Cell-Penetrating Peptides for Potential Use as Gene Transfer Vehicles, *Biomolecules* 2020, *10*(1), 7, https://doi.org/10.3390/biom10010007

[26]. Gelain F., Unsworth L. D., Zhang S., Slow and sustained release of active cytokines from self-assembling peptide scaffolds. *J. Controlled Release* 2010, 145 (3), 231-239. DOI: https://doi.org/10.1016/j.jconrel.2010.04.026.

[27]. Yolamanova M., Meier C., Shaytan A. K., Vas V., Bertoncini C. W., Arnold F., Zirafi O., Usmani S. M., Muller J. A., Sauter D., Goffinet C., Palesch D., Walther P., Roan N. R., Geiger H., et.al, Peptide nanofibrils boost retroviral gene transfer and provide a rapid means for concentrating viruses. *Nature nanotechnology* 2013, 8 (2), 130-6. DOI: 10.1038/nnano.2012.248

[28]. Kasotakis E., Mitraki A., Designed Self-Assembling Peptides as Templates for the Synthesis of Metal Nanoparticles. In Protein Nanotechnology: Protocols, Instrumentation, and Applications, Second Edition, Gerrard, J. A., Ed. Humana Press: Totowa, NJ, 2013; pp 195-202. DOI: 10.1007/978-1-62703-354-1_11.

[29]. Kasotakis, E., Mitraki, A., Silica biotemplating by self-assembling peptides via serine residues activated by the peptide amino terminal group. Biopolymers 2012, 98 (6), 501-509. DOI: 10.1002/bip.22091

[30]. Terzaki K., Kalloudi E., Mossou E., Mitchell E. P., Forsyth V. T., Rosseeva E., Simon P., Vamvakaki M., Chatzinikolaidou M., Mitraki A., Farsari M., Mineralized self-assembled peptides on 3D laser-made scaffolds: a new route toward 'scaffold on scaffold' hard tissue engineering. *Biofabrication* 2013**,** *5* (4). DOI: 10.1088/1758-5082/5/4/045002.

[31]. Jonnalagadda S. V. R., Kokotidou C., Orr A. A., Fotopoulou E., Henderson K. J., Choi C. H.. Lim W. T., Choi S. J., Jeong H. K., Mitraki A., Tamamis P., Computational Design of Functional Amyloid Materials with Cesium Binding, Deposition, and Capture Properties. *The journal of physical chemistry*. B 2018, 122 (30), 7555-7568. DOI: 10.1021/acs.jpcb.8b04103.

[32]. Li D., Jones E. M., Sawaya M. R., Furukawa H., Luo F., Ivanova M., Sievers S. A., Wang W., Yaghi O. M., Liu C., Eisenberg D. S., Structure-based design of functional amyloid materials. *J. Am. Chem. Soc.* 2014, 136 (52), 18044-51. DOI: 10.1021/ja509648u.

[33]. Rufo C. M., Moroz Y. S., Moroz O. V., Stohr J., Smith T. A., Hu X., DeGrado W. F., Korendovych I. V., Short peptides self-assemble to produce catalytic amyloids. *Nat Chem* 2014, 6 (4), 303-9. DOI: 10.1038/nchem.1894.

[34]. Reddy V. S., Natchiar S. K., Stewart P. L., Nemerow G. R., Crystal Structure of Human Adenovirus at 3.5 Å Resolution, *Science,* 2010, Issue 5995, pp. 1071-1075
DOI: 10.1126/science.1187292

[35]. Harrison S. C., Virology. Looking inside adenovirus. *Science*, 2010, 329 (5995): 1026–7, doi:10.1126/science.1194922.

[36]. Jackson K. N., Kahler D. M., Kucharska I., Rekosh D., Hammarskjold M., Smith J. A., Inactivation of MS2 Bacteriophage and Adenovirus with Silver and Copper in Solution and Embedded in Ceramic Water Filters, *Journal of Environmental Engineering*, 2020, 146. 10.1061/(ASCE)EE.1943-7870.0001634.

[37]. Mathot F., Erwan B. Development of a Freeze-Dried Ebola-Expressing Adenoviral Vector Unexpected Findings and Problems Solved. 2018

[38]. Bewley M. C., Springer K., Zhang Y. B., Freimuth P., Flanagan J. M., Structural analysis of the mechanism of adenovirus binding to its human cellular receptor, CAR. *Science* 1999, 286 (5444), 1579-83. DOI: 10.1126/science.286.5444.1579.

[39]. Rentsendorj A., Agadjanian H., Chen X. *et al.* The Ad5 fiber mediates nonviral gene transfer in the absence of the whole virus, utilizing a novel cell entry pathway. *Gene Ther* **12,** 225–237 (2005). https://doi.org/10.1038/sj.gt.3302402

[40]. Krasnykh V., Dmitriev I., Navarro J. G., Belousova N., Kashentseva E., Xiang J., Douglas J. T., Curiel D. T., Advanced Generation Adenoviral Vectors Possess Augmented Gene Transfer Efficiency Based upon Coxsackie Adenovirus Receptor-independent Cellular Entry Capacity, *Cancer Res*, 2000, (60) (24) 6784-6787.

[41]. Mitraki A., Barge A., Chroboczek J., Andrieu J. P., Gagnon J., Ruigrok R. W., Unfolding studies of human adenovirus type 2 fibre trimers Evidence for a stable domain. *Eur. J. Biochem*. 1999, 264 (2), 599-606.

[42]. van Beusechem V., van Rijswijk A., van Es H. et al. Recombinant adenovirus vectors with knobless fibers for targeted gene transfer. *Gene Ther 7*, 1940–1946 (2000) https://doi.org/10.1038/sj.gt.3301323

[43]. Reetz J., Herchenröder O., Pützer B., Peptide-Based Technologies to Alter Adenoviral Vector Tropism: Ways and Means for Systemic Treatment of Cancer. *Viruses,* 2014, 6. 1540-63. 10.3390/v6041540.

[44]. Yamamoto M., Curiel D. T., Current Issues and Future Directions of Oncolytic Adenoviruses, *Molecular Therapy,* 2010, Volume 18, Issue 2, 243-250, https://doi.org/10.1038/mt.2009.266.

[45]. Kokotidou C., PhD Thesis. University of Crete, 2019.

[46]. van Raaij M. J., Schoehn G., Jaquinod M., Ashman K., Burda M. R., Miller S., Identification and crystallisation of a heat- and protease-stable fragment of the bacteriophage T4 short tail fibre. *Biol. Chem.* **2001,** *382* (7), 1049-55.

[47]. Papanikolopoulou K., van Raaij M. J., Mitraki A., Creation of Hybrid Nanorods From Sequences of Natural Trimeric Fibrous Proteins Using the Fibritin Trimerization Motif. In Nanostructure Design: Methods and Protocols, Gazit, E., Nussinov, R., Eds. Humana Press: Totowa, NJ, 2008; pp 15-33. DOI: 10.1007/978-1-59745-480-3_2

[48]. Papanikolopoulou K., Forge V., Goeltz P., Mitraki A., Formation of highly stable chimeric trimers by fusion of an adenovirus fiber shaft fragment with the foldon domain of bacteriophage t4 fibritin. *The Journal of biological chemistry* 2004, 279 (10), 8991-8.

[49]. Kokotidou C, Jonnalagadda S. V. R, Orr A A., Seoane-Blanco M., Apostolidou C. P., van Raaij M. J., Kotzabasaki M., Chatzoudis A., Jakubowski J. M., Mossou E., Forsyth V. T., Mitchell E.P., Bowler M. W., Llamas-Saiz A. L., Tamamis P., Mitraki A, A novel amyloid designable scaffold and potential inhibitor inspired by GAIIG of amyloid beta and the HIV-1 V3 loop, *FEBS Letters* 592 1777-1788 (2018).

[50]. van Raaij M. J., Mitraki A., Lavigne G., Cusack S., A triple beta-spiral in the adenovirus fibre shaft reveals a new structural motif for a fibrous protein. *Nature* 1999, 401 (6756), 935-938.

[51]. Prigipaki A., PhD dissertation. University of Crete, 2017.

[52]. Ferrer-Miralles N., Corchero J. L., Kumar P., Cedano J. A., Gupta K. C., Villaverde A., Vazquez E., Biological activities of histidine-rich peptides; merging biotechnology and nanomedicine. *Microb Cell Fact,* 2011, 10, 101. DOI: 10.1186/1475-2859-10-101.

[53]. Predonzani A., Arnoldi F., López-Requena A., Burrone O. R., In vivo site-specific biotinylation of proteins within the secretory pathway using a single vector system. *BMC Biotechnol*, 2008, 8, 41-41. DOI: 10.1186/1472-6750-8-41.

[54]. Li Y., Sousa R., Novel system for in vivo biotinylation and its application to crab antimicrobial protein scygonadin. *Biotechnol. Lett*, 2012, 34 (9), 1629-35. DOI: 10.1007/s10529-012-0942-3.

[55]. Schatz P., Use of Peptide Libraries to Map the Substrate Specificity of a Peptide-Modifying Enzyme: A 13 Residue Consensus Peptide Specifies Biotinylation in *Escherichia coli*., *Nat Biotechnol* **11,** 1138–1143 (1993). https://doi.org/10.1038/nbt1093-1138

[56]. Gaspar V., Moreira A., de Melo-Diogo D., Costa E., Queiroz J., Sousa F., Pichon C., Correia I., Multifunctional nanocarriers for codelivery of nucleic acids and chemotherapeutics to cancer cells., *Nanobiomaterials in Medical Imaging,* Chapter 6, 2016, https://doi.org/10.1016/B978-0-323-41736-5.00006-6

[57]. Demir B., Guler B., Guler C. E., Güleç K., Yesiltepe O., Odaci D. D., Timur S., Targeting and Imaging of Cancer Cells Using Nanomaterials., *Nanobiomaterials in Medical Imaging,* Chapter 7, 2016, https://doi.org/10.1016/B978-0-323-41736-5.00007-8

[58]. "Polymerase Chain Reaction (PCR)", *National Center for Biotechnology Information, U.S. National Library of Medicine.*